was shown to inhibit in vitro and in vivo splicing and promote pre-mRNA (unspliced mRNA) accumulation by binding to SF3b. Furthermore, spliceostatin leaks pre-mRNA into the cytosol, where it is translated. This study showed that the inhibition of pre-mRNA splicing during early steps involving SF3b allows unspliced mRNA leakage and translation.[16] Interestingly, SF3b was also identified as a target of pladienolide by Mizui et al.[17] Pladienolide was isolated from the fermentation broth of *Streptomyces platensis* Mer-11107 as an anti-tumor macrolide, which was discovered by using a cell-based reporter gene expression assay controlled by the human vascular endothelial growth factor promoter.[24–26] They first synthesized fluorescence-tagged pladienolide to monitor the intracellular localization of the target protein. HeLa cells treated with fluorescence-tagged pladienolide showed localization of the pladienolide to the granular structure in the nuclei. These granules overlapped with the localization of splicing factor SF3b. Furthermore, SF3b was confirmed to be a target of pladienolide by purification of the binding protein using biotinylated-pladienolide. Like spliceostatin, pladienolide also inhibited in vivo splicing. These two small molecules showed anti-tumor activity, and these studies suggest that the SF3b complex is a potential anti-tumor drug target. Indeed, pladienolide is now in phase I clinical trials.

2.2. Affi-Gel tag

As well as the biotin affinity tag, purification of the target protein using Affi-gel is also an excellent strategy. The Affi-gel matrix is able to directly link to the small molecule of interest. Thus, compared with the biotin-affinity tag, the number of non-specific interactions with the affinity matrix is reduced. Here, we highlight target proteins of several bioactive small molecules which were identified by using the Affi-gel system. Embryonic stem cells (ES cells) provide an excellent in vitro system for the study of early development and human disease. However, the mechanisms that govern their self-renewal and differentiation are largely unknown. Thus, small molecules that maintain self-renewal or promote differentiation would be useful discoveries to understand self-renewal and differentiation mechanisms. SC1, a derivative of 3,4-dihydropyrimido[4,5-*d*]pyrimidine, was identified to maintain the undifferentiated phenotype of mouse ES (mES) cells by Ding et al.[27] To identify the cellular target of SC1, SC1 was linked at the N1 position to an agarose affinity matrix via a polyethylene glycol linker. Whole-cell lysates of mES cells were incubated with this affinity matrix and the binding proteins were purified and analyzed by liquid chromatography–mass spectrometry (LC/MS). As a result, the SC1-binding proteins were identified as ERK1 and RasGAP. Direct binding of SC1 to ERK1 or RasGAP was confirmed by surface plasmon resonance (SPR). Further biochemical and cellular experiments suggested that SC1 works through dual inhibition of ERK1 and RasGAP.

The mammalian target of the rapamycin (mTOR) signaling network is crucial for the regulation of cell growth in response to both growth factors and nutrients. Although carbon and nitrogen sources, such as glucose and glutamine, are primary stimuli of mTOR, the mechanism by which they stimulate the mTOR pathway are still unknown. Thus, Schreiber and co-workers screened small molecule modulators of mTOR signaling.[28] From a collection of ~20,000 compounds in the library, they discovered quinostatin as an inhibitor of mTOR signaling. Since the molecular target of quinostatin was unknown, they carried out affinity chromatography purification to identify this target protein. An analog of quinostatin was prepared by attaching a polyethylene glycol linker, and this polyethylene glycol-modified quinostatin was immobilized to agarose beads. To isolate the target protein of quinostatin, MCF7 cell lysates were incubated with the affinity reagent. After LC/MS analysis, the target protein of quinostatin was found to be the catalytic subunit of the class Ia PI3Ks.

Similarly, QS11, a purine derivative, that synergizes with a Wnt-3a ligand in the activation of Wnt/β-catenin signal transduction, was shown to bind the GTPase activating protein of ADP-ribosylation factor 1 (ARFGAP1) by using the Affi-Gel system. ARFGAPs form a family of GTPase-activating proteins that regulate the small GTPase ADP-ribosylation factors (ARFs). ARFGAPs promote ARF inactivation by stimulating GTP hydrolysis, whereas guanine nucleotide exchange factors of ARF (ARFGEFs) catalyze the formation of active GTP-bound ARFs. QS11 significantly increased the levels of GTP-bound ARFs in NIH3T3 cells, suggesting that QS11 inhibited ARFGAPs. It has been reported that the activation of ARFs promotes the dissociation of membrane-bound β-catenin.[29] Thus, QS11 was suggested to inhibit ARFGAP, thereby leading to an increase in activated ARF and subsequent β-catenin translocation. The released β-catenin accumulates and translocates to the nucleus when cells are stimulated with Wnt-3a.

2.3. Phage display

Terpestacin was identified to inhibit the functional response to hypoxia of human umbilical vein endothelial cells in vitro and angiogenesis within the embryonic chick chorioallantonic membrane in vivo.[30] Furthermore, terpestacin has been shown to inhibit hypoxia-induced HIF-1α and VEGF expression. These results indicate that terpestacin inhibits hypoxia-induced tumor angiogenesis via the inhibition of HIF-1α-mediated VEGF expression. To better understand the cellular mechanisms of its anti-angiogenic activity, Kwon et al. aimed to identify the target molecule for terpestacin by using phage display biopanning.[31] They first synthesized biotinylated-terpestacin, which was then immobilized on a streptavidin-coated well plate, and four rounds of phage biopanning were conducted using T7 phages expressing functional human cDNA libraries. As a result, UQCRB, a 13.4 kDa subunit of complex III in the mitochondrial respiratory chain,[32] was identified as a terpestacin-binding protein. Knockdown of UQCRB by siRNA resulted in inhibition of hypoxia-induced HIF-1α accumulation and VEGF expression in HT1080 cells. These results suggest that UQCRB plays a key role in the cellular oxygen-sensing and transduction systems. This study provided a new insight into the oxygen-sensing role of UQCRB in mitochondrial complex III.

2.4. Click chemistry

Affinity purification using biotin- or fluorescence-tagged small molecules is a powerful tool for target identification, but biotin- or fluorescence-modifications at the biologically active site of interest can result in a complete loss of activity. To overcome this problem, azide alkyne Huisgen cycloaddition chemistry (a common technique within so-called 'click chemistry') was adapted for target identification. The advantage of using this approach is that minimal structural modification is introduced to the small molecule of interest, without any loss of biological activity. Once the alkyne-derivatized small molecule is covalently bound to its target protein, a tag (e.g., fluorescein-azide or rhodamine-azide) can subsequently be attached via click chemistry.

Click chemistry was first adapted for live cell labeling by Bertozzi et al.[33] Jurkat cells were incubated with Ac_4-ManNAz to introduce SiaNAz residues into their cell-surface glycoproteins. Then, the azide-modified cell-surface glycoproteins were labeled with biotinylated cyclooctyne by using click chemistry. Therefore, the azide-modified cell-surface glycoproteins could be analyzed by flow cytometer with FITC-avidin. This is the first report to employ the reaction for the selective chemical modification of living cells.

Pezacki et al. used click chemistry reactions to identify the target protein of origamicin, an inhibitor of HCV replication.[34] Small molecules that interfere with host-viral interactions are potentially powerful tools for elucidating the molecular mechanisms of pathogenesis and defining new strategies for therapeutic development. Thus, Pezacki et al. screened for HCV replication inhibitors in their established ABA ((+)-S-abscisic acid) library based on the plant hormone ABA, a carotenoid-derived sesquiterpene. As a result, origamicin was identified as an HCV replication inhibitor. Because origamicin has an alkyne moiety in its structure, they exploited it to conjugate both rhodamine for in-gel fluorescence experiments and biotin for affinity chromatography experiments by using click chemistry. The purified protein from using biotinylated-origamicin was identified via LC–MS/MS as protein disulfide isomerase (PDI).

Stockwell et al. screened an inhibitor that suppresses cell death induced by polyglutamine-expanded huntingtin exon 1 (a cell-based model of Huntington's disease) from a 68,887 small-molecule library containing natural products and synthetic small molecules.[35] One hit was small molecule 16F16, and Stockwell et al. synthesized both biotin- and fluorescein-tagged 16F16. However, the modified 16F16 lost its biological activity, so they then used click chemistry. Lysates of PC12 were prepared and incubated with alkyne-derivatized 16F16 to bind to a target protein. Alkyne-derivatized 16F16 was coupled to rhodamine-azide via a click chemistry reaction. Next, fluorescent-tagged target proteins were affinity-purified, analyzed by SDS–PAGE and identified by MS as rat PDI (protein disulfide isomerase) precursors, PDIA1 and PDIA3. Expression of polyglutamine-expanded huntingtin exon 1 in PC12 cells caused PDI to concentrate at ER-mitochondrial junctions and triggered apoptosis via mitochondrial outer-membrane permeabilization. These studies demonstrated a novel strategy for identifying target proteins of small molecules.

2.5. Photo-crosslink

An additional method for overcoming the problem of a loss of biological activity of small molecules due to the presence of an affinity tag is photo-crosslink. Osada et al. developed this new method, which enables the introduction of a variety of small molecules onto solid supports through a photoaffinity reaction.[36] In this method, aryldiazirine groups covalently attached to solid supports are transformed upon UV irradiation into highly reactive carbenes, which are expected to bind to or insert irreversibly into proximal small molecules in a functional-group-independent manner. Osada et al. applied this method to methyl-gerfelin,[37] which had been found to suppress osteoclastogenesis. To understand the molecular mechanism by which this occurred, methyl-gerfelin was immobilized on agarose beads via a photoaffinity linker which they had developed. Binding proteins were purified and analyzed by MALDI-TOF MS, and glyoxalase I (GLO1) was identified as a methyl-gerfelin-binding protein. GLO1 knockdown interfered with osteoclast generation, and methyl-gerfelin competitively inhibited GLO1 enzymatic activity. These results suggest that methyl-gerfelin targets GLO1, resulting in the inhibition of osteoclastogenesis.

2.6. FG beads

Affinity purification using conventional matrices has several disadvantages, including nonspecific binding of irrelevant proteins to the affinity matrices and instability of these matrices. To overcome these issues, Handa and co-workers designed nonporous and physically stable, submicron-sized particles for affinity chromatography. In order to avoid nonspecific protein binding and to allow easy surface modification, they used polymer materials as components of the particles so that their surfaces possessed moderate hydrophilicity and an appropriate functional group. Based on these considerations, they developed high-performance affinity magnetic beads (FG beads)[38] and aimed to identify the target protein of thalidomide by using FG beads. Thalidomide was sold as a sedative in many countries and was often prescribed to pregnant women as a treatment for morning sickness. However, use of thalidomide causes multiple birth defects such as limb, ear, cardiac, and gastrointestinal malformations.[39–41] Despite considerable effort, little is known about the mechanisms underlying these developmental defects caused by thalidomide. Handa et al. identified cereblon (CRBN) as a thalidomide-binding protein by using FG beads.[42] CRBN was originally identified as a candidate gene for autosomal recessive mild mental retardation.[43] Although CRBN was reported to interact with DDB1,[44] which is a component of E3 ubiquitin ligase complexes containing Cullin 4 (Cul4A and Cul4B),[45] the functional relevance of this interaction remained unclear. Based on this information, they demonstrated that CRBN forms an E3 complex with DDB1 and Cul4A. Furthermore, thalidomide inhibited E3 ubiquitin ligase activity of the CRBN-containing complex due to its binding to CRBN. Next, to investigate whether the teratogenic effect of thalidomide could be observed in CRBN-knockdown animals, Handa et al. used zebrafish. CRBN-knockdown zebrafish by use of morpholino oligonucleotides exhibited specific defects in fin and otic vesicle development, which was a similar phenotype to those of thalidomide-treated embryos. Thus, thalidomide was shown to exert its teratogenic effects by binding to CRBN and inhibiting the associated ubiquitin ligase activity.

3. Indirect approach

Affinity chromatography is the most used and most successful method for identifying biological targets of multiple small molecules of interest. However, target identification using affinity chromatography begins with a structure–activity relationship (SAR) study, because we have to know which site(s) are nonessential to use as points of attachment to an affinity tag (e.g., biotin) or solid matrix (e.g., Affi-Gel agarose beads). Therefore, the primary limitation of affinity chromatography is the need to synthesize derivatives of small molecules. SAR studies are time-consuming and require extensive medicinal chemistry expertise. Furthermore, since biologically-active small molecules demonstrate vast structural diversity and complexity, many small molecules cannot be modified without affecting bioactivity, or cannot be easily obtained or synthesized in quantities large enough to permit SAR and subsequent studies. Because of these issues, target identification of small molecules using affinity chromatography is severely limited. This section highlights several 'Indirect Approaches' to overcome the limitations of the previously listed 'Direct Approaches' (Figs. 1B and 3).

3.1. DARTS (drug affinity responsive target stability)

To overcome the limitations of affinity chromatography described above, Huang and co-workers developed DARTS (Fig. 4). The strategy of DARTS is based on the principle that binding of drugs will stabilize target proteins, either globally or locally, for example, in a specific conformation or simply by masking protease recognition sites, thereby reducing the protease sensitivity of the target protein.[46–48] Thus, Huang et al. hypothesized that this could be exploited for target identification without requiring modification or immobilization of the small molecules. As a proof-of-principle, they first demonstrated that DARTS could identify FKBP12 as an FK506-binding protein.[49] Next, they aimed to apply DARTS to identify a molecular target of resveratrol, a small

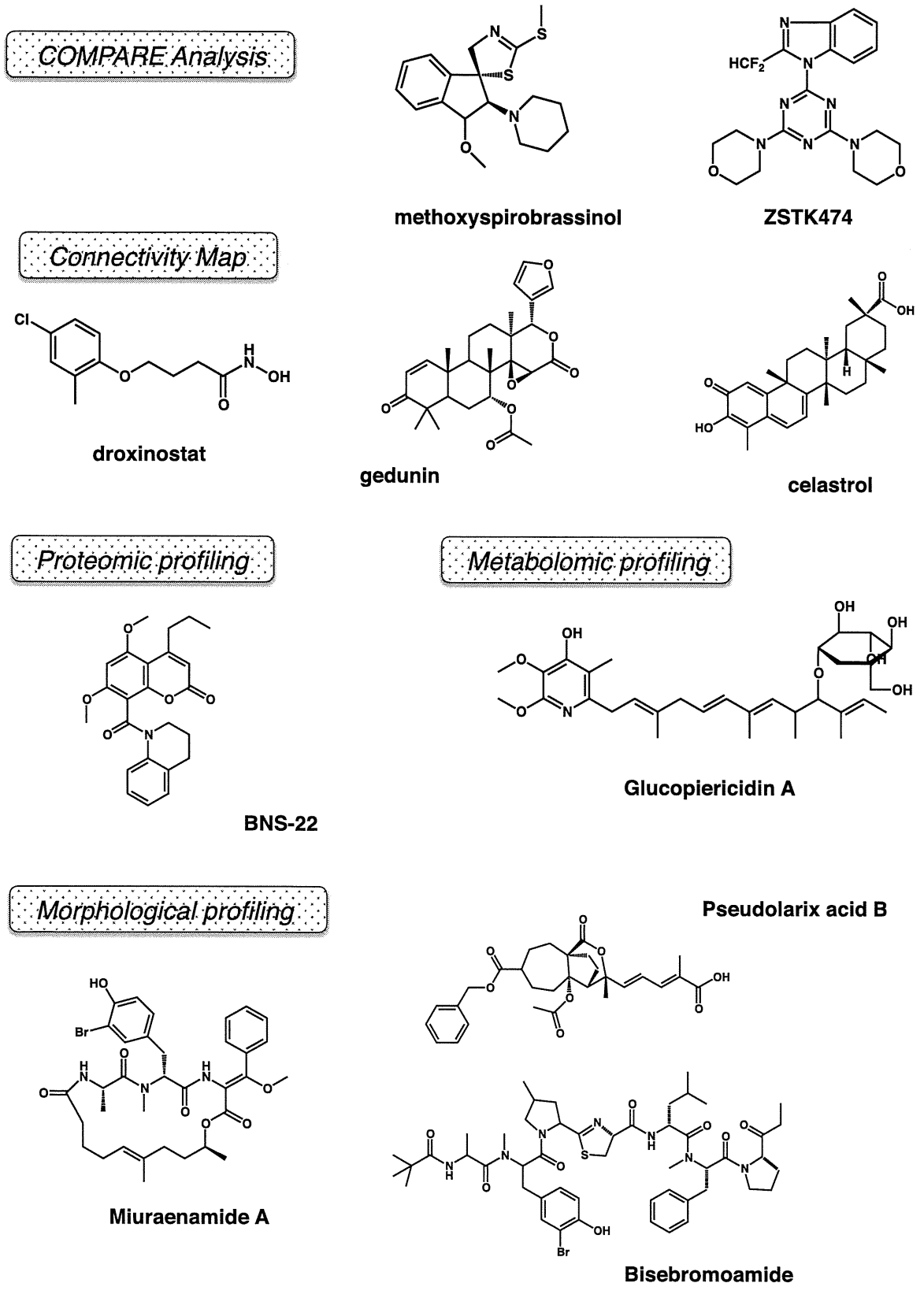

Figure 3. Structure of small molecules whose targets were identified by the 'Indirect Approach'.

molecule in red grapes and wine known for various health benefits including lifespan extension.[50]

Yeast cell lysates or human HeLa cell lysates were treated with resveratrol in vitro, followed by thermolysin digestion and silver staining after separation by SDS–PAGE. Bands of resveratrol-treated lysate protected from thermolysin digestion were analyzed by MS, and were identified as eIF4A (eukaryotic translation initiation factor 4A), a component required for the binding of mRNA to

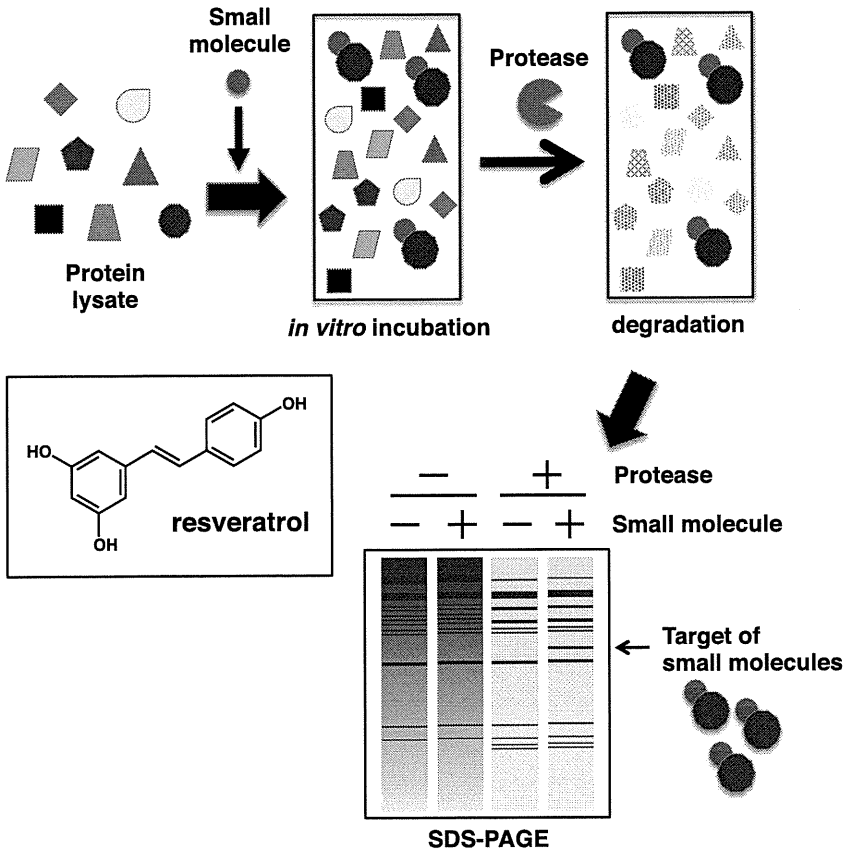

Figure 4. Schematic illustration of DARTS. Yeast or mammalian cultured cell lysates were prepared and treated with small molecules of interest in vitro, followed by protease digestion and silver staining after separation by SDS–PAGE.

40S ribosomal subunits. Purified wild-type eIF4A could be protected by resveratrol from proteolysis, suggesting that resveratrol directly bound to eIF4A. Furthermore, to address whether eIF4A is a target of resveratrol in vivo, they investigated the effect of resveratrol on EMCV IRES-mediated and HCV-mediated translation. Since it has been demonstrated that eIF4A is required for EMCV IRES-mediated translation but not HCV IRES-mediated translation, it follows that resveratrol inhibited EMCV-mediated but not HCV-mediated translation in HEK293 cells. These results indicated that resveratrol inhibited the biological function of eIF4A in vivo. On the other hand, because resveratrol extends lifespan,[50] they asked whether eIF4A is required for resveratrol's longevity effect. Whereas resveratrol lengthens the lifespan of wild-type N2 worms, this longevity effect is lost in eIF4A knockdown worms. These data suggested that eIF4A is a physiological target of resveratrol. Because DARTS does not require labeled small molecules and instead uses 'native' small molecules for binding, it is not limited by chemistry and can potentially be used for any small molecules.

3.2. Profiling

Apart from traditional target identification techniques such as affinity chromatography, new tools have emerged that can significantly aid mechanism elucidation efforts. The development of pattern matching algorithms that compare transcription profiles, drug susceptibility profiles, or morphological profile data, for example, to analogous data on compounds with known cellular targets, allow for mechanistic insights without the need to synthesize chemically-modified probes. Therefore, we next focus on new approaches using these pattern matching and chemical genomic tools.

3.3. COMPARE analysis

The National Cancer Institute established a panel of 60 human cancer cell lines (NCI60) derived from various organs. In a COMPARE analysis, the pattern of toxicity of small molecules to the NCI60 cell line panel is compared. Small molecules that have similar patterns of toxicity are highly correlated in the COMPARE algorithm; such a result suggests the small molecules have a similar mechanism of action, and indeed COMPARE has been successfully used in target identification studies. For example, 2-piperidyl analogues of natural indole phytoalexins, 1-methoxyspirobrassinols, and *N*-((1-benzyl-1*H*-1,2,3-trizol-4-yl)methyl)arylamide were reported to decrease intracellular glutathione levels[51] and inhibit tubulin polymerization,[52] respectively. Phytoalexins are small molecules naturally produced by plants. Various indole phytoalexins have been shown to exhibit anti-tumor activities. However, the anti-proliferative activity of most indole phytoalexins had been limited to certain cancer cells, and their mode of action has not been elucidated. Therefore, in order to achieve higher potency, new derivatives of indole phytoalexins have been synthesized. McDonald et al. synthesized 2-piperidyl analogues of indole phytoalexins, *cis*-1-Boc-, *trans*-1-Boc-, *cis*-1-methoxy- and *trans*-1-methoxy-2-deoxy-2-(1-piperidyl)spirobrassinols, and these derivatives exhibited a more favorable growth-inhibitory effect on some cancer cells than their parent compounds. Furthermore, to elucidate their mode of action, McDonald et al. performed COMPARE analysis with the NCI60 cell line panel. As a result, the profiles of their synthesized indole phytoalexins showed similar patterns with small molecules that deplete intracellular glutathione level, such as *N*-methylformamide and L-buthionine sulfoximine (BSO). Indeed, their synthesized indole phytoalexins decreased intracellular glutathione levels in

MCF-7 cells. Since glutathione is often involved in the resistance of cancer cells to radio- and chemotherapy, these small molecules with remarkable glutathione-depleting potency may be developed as radio- or chemo-sensitizing agents. A series of *N*-((1-benzyl-1*H*-1,2,3-trizol-4-yl)methyl)arylamides are synthetic derivatives of mycobactin S, a natural product produced by *Mycobacterium smegmatis* that exhibits anti-tuberculosis activity.[53] Moller et al. found that their synthesized derivatives showed anti-proliferative effects against human cancer cell lines. To evaluate the mode of action of *N*-((1-benzyl-1*H*-1,2,3-trizol-4-yl)methyl)arylamides, they performed COMPARE analysis with the NCI60 cell line panel. COMPARE analysis revealed that *N*-((1-benzyl-1*H*-1,2,3-trizol-4-yl)methyl)arylamides correlated with paclitaxel, vinblastine, and rhizoxin, all of which affect microtubule polymerization. Although further studies confirmed that *N*-((1-benzyl-1*H*-1,2,3-trizol-4-yl)methyl)arylamides inhibited microtubule polymerization in vitro and in vivo and induced G2/M cell cycle arrest, the mechanism by which *N*-((1-benzyl-1*H*-1,2,3-trizol-4-yl)methyl)arylamides inhibit microtubule polymerization still remains unclear.

Similar to the NCI60 cell line panel, Yamori et al. established a panel of 39 human cancer cell lines (termed JFCR39) coupled to a drug activity database. By using the JFCR39 database, they found that ZSTK474 exhibited similar responses to the PI3K inhibitor LY294002, suggesting that ZSTK474 is a new PI3K inhibitor.[54] Indeed, ZSTK474 was found to directly inhibit PI3K activity more efficiently than the PI3K inhibitor LY294002. Molecular modeling of the PI3K-ZSTK474 complex indicated that ZSTK474 could bind to the ATP-binding pocket of PI3K. These studies strongly suggest that this approach can be used to predict the molecular target or the mode of action of small molecules.

3.4. Connectivity Map database

Whole-genome transcript profiling has emerged as powerful tool to investigate the effects of small molecules on cells. The Connectivity Map database, developed at the Broad Institute, is a publicly accessible database comprised of gene expression data of cells treated with small molecules.[55] The transcript profile data of a compound of interest is compared to analogous data that has been collected on hundreds of small molecules with known molecular targets. The Connectivity Map database has been utilized in mode-of-action studies of several small molecules. For example, droxinostat was first identified as sensitizing malignant cells to the CH-11 Fas-activating antibody.[56] However, the Connectivity Map database revealed that the transcript profile of droxinostat showed a similar response to that of the HDAC inhibitors vorinostat and trichostatin A. Further cell-based and in vitro assays showed that droxinostat is a novel HDAC inhibitor that is selective for HDAC3, HDAC6, and HDAC8 through its hydroxamic acid moiety. To further explore the effects of HDAC inhibitions on Fas sensitization, Schimmer et al. knocked down HDACs with shRNA. As a result, HDAC8 knockdown enhanced sensitivity to Fas. Furthermore, droxinostat or HDAC8 knockdown was shown to decrease FLIP mRNA, a caspase-8 inhibitory protein. These results suggested that droxinostat decreased FLIP via HDAC inhibition, which resulted in sensitization to Fas-induced apoptosis. However, it is unclear whether HDACs inhibition by droxinostat would directly or indirectly decrease FLIP expression. Other examples include gedumin and celastrol. These two small molecules were identified as inhibitors of androgen receptor (AR)-activated signaling in prostate cancer by a high-throughput cell-based screening.[57] The Connectivity Map database revealed that these compounds were predicted to have a similar mode of action to the heat shock protein 90 (HSP90) inhibitors geldanamycin, 17-dimethylamino-geldanamycin and 17-allylaminogeldanamycin. It has been reported that the androgen receptor is a client of HSP90, and HSP90 inhibitors induced AR degradation. Thus, gedunin and celasteol were predicted to inhibit AR signaling by inhibiting HSP90. Indeed, these two compounds induced the down-regulation of AR and several other HSP90 client proteins. Furthermore, these two small molecules inhibited ATP binding to HSP90. However, since gedunin and celasteol did not compete for the ATP-binding site, gedunin and celasteol seem to have distinct mechanisms from geldanamycin. These studies suggested that the Connectivity Map database could also be used to predict the molecular target or the mode of action of small molecules.

3.5. Proteomic profiling

Compared with gene expression profiling like the Connectivity Map database which can simultaneously measure the expression of more than 20,000 genes, proteome analysis provides us with only ~1000 protein spots. However, two-dimensional gel electrophoresis (2DE) analyses often show us any change in molecular weight or isoelectric point of proteins after posttranslational modification as a clear mobility shift of protein spots. Because biologically active small molecules affect cellular processes and induce changes in both the expression level and modification of proteins, proteome profiling is an informative approach for investigating the effects of a small molecule. Osada and co-workers developed a new proteomic profiling system to predict the target protein of small molecules of interest.[58] To compare the proteomic pattern with small molecules whose targets are known, HeLa cells treated with each small molecule were analyzed by 2D-DIGE, and hierarchical clustering was performed. For example, radicicol and geldanamycin (structurally different HSP90 inhibitors), showed a similar proteome pattern, suggesting that this proteomic profiling system discriminates small molecules by mechanism of action. Indeed, the proteomic profiling analysis of BNS-22, a chemically synthesized derivative of the natural plant product GUT-70, showed that BNS-22 belongs to the same cluster as ICRF-193, a DNA topoisomerase II (TOP2) catalytic inhibitor. Further biochemical studies confirmed that BNS-22 targets and acts as a catalytic inhibitor of TOP2.[59]

3.6. Morphological profiling

A recent and rapidly developing technology is high content screening (HCS) that combines automated microscopy with image analysis, enabling phenotypic profiling of small molecules based on the activity of cells visualized by fluorescence cytology. Feng et al. introduced factor analysis as a data-driven tool for defining cell phenotypes and profiling small molecule activity.[60] They used a high-content image assay to screen and profile a library of 6547 small molecules derived from a diversity library (21%), a natural products library (58%) and a library of known bioactive small molecules (21%); all small molecules were assayed in HeLa cells to monitor cell proliferation, and to profile their cell cycle phenotype, using fluorescent probes for DNA (Hoechst 33342 dye), mitosis (anti-phosphoH3) and DNA replication (EdU; 5-ethyl-2-deoxyuridine). Images were automatically acquired and at least 500 cells were scored per treatment. They found that six factors (nuclear size, DNA replication, chromosome condensation, nuclear morphology, EdU texture, and nuclear shape) are sufficient to describe the biological responses. Profiling the small molecule library using these six factors resulted in the clustering of hits into seven phenotypic categories. Feng et al. then compared the phenotypic profiles, chemical similarity and predicted protein-binding activity of these small molecules. For instance, within the subcluster from the mitotic arrest phenotype, which is primarily characterized by high chromosome condensation, the authors observed four distinct

groups of structurally related small molecules; colchicine derivatives, a set of novel kinase inhibitors, quinolone derivatives and a pseudolarix acid B derivative. All of these small molecules have been reported to affect microtubules polymerization.[61–63] Indeed, they demonstrated depolymerization of microtubules and mitotic arrest in cells treated with each of the colchicine, quinolone and pseudolarix acid B derivatives.

Further cell morphological profiling has revealed bisebromoamide and miuraenamide A as actin filament stabilizers. Uesugi et al. used automated high-content image analysis to evaluate the morphology of cells exhibiting nuclear protrusion.[64] Actin-targeting small molecules decreased cytoplasmic area up to ~70%, and increased the distance between the centroid of the nucleus and the centroid of the entire cell. When those two parameters were plotted against each other, points for the seven known actin-targeting small molecules, cytochalasin D,[65] doliculide,[66] jasplakinolide,[67] latrunculin A,[68] mycalolide B,[69] seragamide A,[70] and swinholide A,[71] were clustered together. Based on this morphological profiling, the target of bisebromoamide and miuraenamide A, marine natural products whose targets were previously unknown,[72–75] were predicted to be actin stabilization. Indeed, they showed that bisebromoamide and miuraenamide A stabilized actin filaments in vitro, and fluorescein-conjugated bisebromoamide localized specifically to actin filaments in cells.

3.7. Metabolomics profiling

Metabolomic technologies have advanced tremendously in recent years, and capillary electrophoresis time-of-flight mass spectrometry (CE-TOFMS) has emerged as a powerful new tool for the comprehensive analysis of cellular metabolites.[76,77] The use of CE-TOFMS to understand global metabolism at the system level has become widespread.[78–81] Analysis of the metabolome with CE-TOFMS also reveals metabolic changes induced by small molecules. Thus, despite a lack of reports describing the identification of chemical inhibitor targets using metabolomic analysis, such efforts would be worthwhile. We screened bioactive compounds that inhibit cellular filopodia protrusion in carcinoma. Filopodia

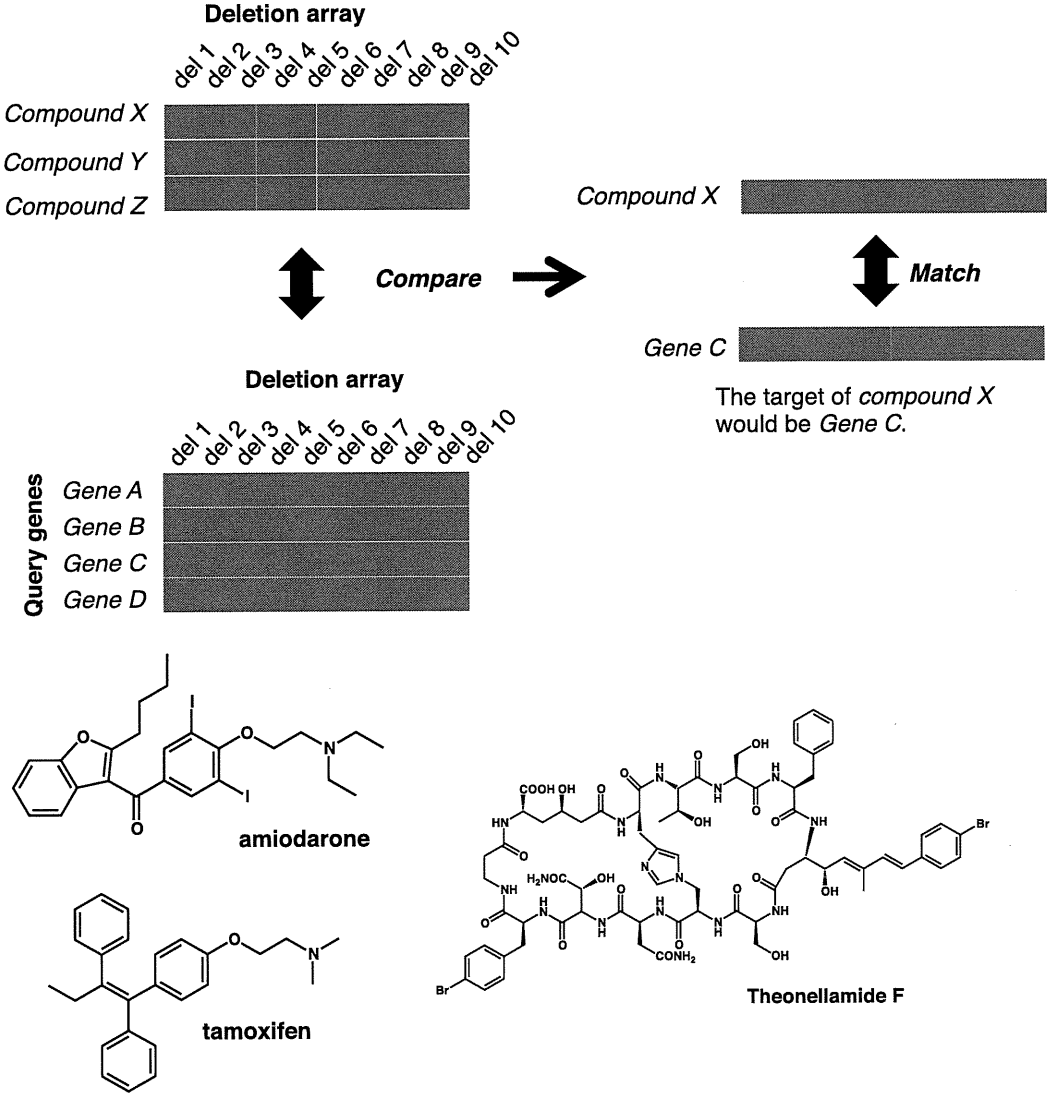

Figure 5. Comparison of a chemical-genetic profile to a compendium of genetic interaction (synthetic lethal) profiles could identify pathways and target genes of small molecules. Conceptually, the comparison of a chemical-genetic profile to the genetic interaction (synthetic lethal) profiles should identify the pathways and targets inhibited by small molecule treatment. For example, deletion mutants del2, del5, del6 and del8 are hypersensitive to compound X and a mutation in query *gene* C leads to a fitness defect when combined with deletion alleles del2, del5, del6 and del8. Here, the chemical-genetic profile of compound X resembles the genetic profile of *gene* C, thereby identifying the product of *gene* C as a putative target of compound X.

are spike-like cell membrane projections contributing to tumor metastasis; however, the molecular mechanisms controlling filopodia protrusion are complicated and unclear.[82,83] Thus, the discovery of a filopodia inhibitor and its molecular target which could be employed in chemical genetic studies may lead to a fuller understanding of filopodia, contributing to the treatment of tumor metastasis. In the course of screening filopodia protrusions from microbial origin, glucopiericidin A was isolated. Biochemical studies raised the possibility that glucopiericidin A would be an inhibitor of glycolysis. To address whether glucopiericidin A actually perturbs glycolysis, the effect of glucopiericidin A on global metabolism and on glycolysis was assessed by measuring the metabolome using CE-TOFMS. CE-TOFMS provided strong evidence that glucopiericidin A suppresses glycolysis by functionally targeting the glucose transporter. Our results represent a success of molecular target identification using metabolomics analysis.[84]

3.8. Chemical-genetic profiling in yeast

In yeast *Saccharomyces cerevisiae*, ~6000 potential genes have been characterized by the genome sequencing project. As each gene has been deleted, ~1000 essential genes and ~5000 viable deletion mutants were identified. Boone et al. generated a compendium of 'chemical-genetic interaction' profiles from scoring ~5000 viable yeast haploid deletion mutant strains for hypersensitivity to a diverse set of small molecules.[85] In addition, they also generated 'genetic interaction (synthetic lethal)' profiles by testing viabilities in each double gene-mutant combination. Conceptually, the comparison of a chemical-genetic profile to the genetic interaction (synthetic lethal) profile should identify the pathways and targets inhibited by small molecule treatment (Fig. 5).

Boone et al. generated chemical-genetic profiles for 82 different conditions by testing the collection of viable yeast haploid deletion mutants for hypersensitivity to 82 small molecules, including 75 synthetic and natural products and 7 crude antifungal extracts derived from different marine sponges and microorganisms.[86] The set of chemical-genetic profiles, visualized by two-dimensional hierarchical clustering, revealed that small molecules with similar cellular effects showed similar chemical-genetic profiles. Examples include (i) actin binding agents latrunculin B[87] and cytochalasin A;[88] (ii) cell wall synthesis inhibitors staurosporine, which targets protein kinase C, a regulator of a MAP kinase cascade involved in cell wall metabolism,[89] and caspofungin, which inhibits 1,3 β-glucan synthase;[90] (iii) radicicol and geldanamycin—although structurally unrelated, both act as highly selective inhibitors of Hsp90 function through their ability to bind within the ADP/ATP binding pocket of the chaperone.[91] Interestingly, the chemical-genetic interactions of amiodarone, an antifungal and anti-arrhythmic small molecule, clusters with tamoxifen, a competitive inhibitor of estradiol binding to the estrogen receptor and a common breast cancer drug. This is notable, as the antifungal activity of amiodarone is the perturbation of calcium homeostasis,[92] and tamoxifen seems to produce an increase in cytosolic Ca^{2+} in yeast. Indeed, both amiodarone and tamoxifen triggered the reporter activity driven by calcineurin-dependent response element (CDRE), suggesting that tamoxifen is a potent activator of calcineurin signaling. Furthermore, two natural product extracts (prior to purification of the active component) that were derived from different organisms and diverse locations, from a sea cucumber from the Commonwealth of Dominica and an Indonesian marine sponge, showed highly similar chemical-genetic profiles. After purification, the active components were identical to stichloroside[93] and theopalauamide,[94] respectively. Both of the purified small molecules display chemical-genetic profiles resembling those of their crude extracts, suggesting that chemical-genetic profiling is an effective means for functional classification of natural product extracts. Taken together, Boone et al. demonstrated the potential for integration of chemical-genetic profiles and genetic interaction profiles to provide information about the pathways and targets affected by bioactive small molecules.

Another example was reported by Yoshida et al.[95] Theonellamides are members of a unique family of bicyclic dodecapeptides isolated from a marine sponge, *Theonella* sp. These small molecules show broad antifungal activity as well as moderate cytotoxicity in mammalian cells.[96,97] Despite screens for binding proteins using theonellamide A affinity beads, their target molecules remain unknown.[98] Therefore, to evaluate the mode of action of theonellamide, Yoshida et al. generated a chemical-genomic profile of theonellamide F, bicyclic peptides derived from a marine sponge, using a collection of fission yeast strains in which each open reading frame (ORF) is expressed under the control of an inducible promoter (fission yeast ORFeome overexpression strain collection).[99,100] The overexpression strains were exposed individually to theonellamide F and a compendium of 10 reference small molecules with known targets at various concentrations. Strains showing a significantly altered sensitivity compared to the control strain were selected. Cluster analysis of the Gene Ontology (GO) terms associated with the genes that alter small molecule sensitivity suggested a mechanistic link between theonellamide and 1,3-β-D-glucan synthesis. Overproduction of 1,3-β-D-glucan was induced by theonellamide F in a Rho1-dependent manner. Furthermore, by using a fluorescent theonellamide derivative, theonellamides were shown to specifically bind in vitro to 3β-hydroxysterols, including ergosterol, and cause membrane damage. Taken together, these results show that theonellamides are a new class of sterol-binding molecules that induce membrane damage and activate Rho1-mediated 1,3-β-D-glucan synthesis.

Acknowledgements

We are grateful to Ms. Yukiko Sasazawa, Ms. Satoko Shinjo, Mr. Kohta Yamamoto, Mr. Shigeyuki Magi, and Mr. Takahiro Fujimaki for supporting some of our work.

References and notes

1. Pandey, A.; Mann, M. *Nature* **2000**, *405*, 837.
2. Alaimo, P. J.; Shogren-Knaak, M. A.; Shokat, K. M. *Curr. Opin. Chem. Biol.* **2001**, *5*, 360.
3. Zheng, X. F.; Chan, T. F. *Drug Discovery Today* **2002**, *7*, 197.
4. Kino, T.; Hatanaka, H.; Hashimoto, M.; Nishiyama, M.; Goto, T.; Okuhara, M.; Kohsaka, M.; Aoki, H.; Imanaka, H. *J. Antibiot. (Tokyo)* **1987**, *40*, 1249.
5. Siekierka, J. J.; Hung, S. H.; Poe, M.; Lin, C. S.; Sigal, N. H. *Nature* **1989**, *341*, 755.
6. Liu, J.; Farmer, J. D., Jr.; Lane, W. S.; Friedman, J.; Weissman, I.; Schreiber, S. L. *Cell* **1991**, *66*, 807.
7. Omura, S.; Fujimoto, T.; Otoguro, K.; Matsuzaki, K.; Moriguchi, R.; Tanaka, H.; Sasaki, Y. *J. Antibiot. (Tokyo)* **1991**, *44*, 113.
8. Fenteany, G.; Standaert, R. F.; Lane, W. S.; Choi, S.; Corey, E. J.; Schreiber, S. L. *Science* **1995**, *268*, 726.
9. Jensen, T. J.; Loo, M. A.; Pind, S.; Williams, D. B.; Goldberg, A. L.; Riordan, J. R. *Cell* **1995**, *83*, 129.
10. Lee, D. H.; Goldberg, A. L. *Trends Cell Biol.* **1998**, *8*, 397.
11. Hart, C. P. *Drug Discovery Today* **2005**, *10*, 513.
12. Galat, A.; Lane, W. S.; Standaert, R. F.; Schreiber, S. L. *Biochemistry* **1992**, *31*, 2427.
13. Choi, Y.; Shimogawa, H.; Murakami, K.; Ramdas, L.; Zhang, W.; Qin, J.; Uesugi, M. *Chem. Biol.* **2006**, *13*, 241.
14. Falsey, R. R.; Marron, M. T.; Gunaherath, G. M.; Shirahatti, N.; Mahadevan, D.; Gunatilaka, A. A.; Whitesell, L. *Nat. Chem. Biol.* **2006**, *2*, 33.
15. Kahsai, A. W.; Cui, J.; Kaniskan, H. U.; Garner, P. P.; Fenteany, G. *J. Biol. Chem.* **2008**, *283*, 24534.
16. Kaida, D.; Motoyoshi, H.; Tashiro, E.; Nojima, T.; Hagiwara, M.; Ishigami, K.; Watanabe, H.; Kitahara, T.; Yoshida, T.; Nakajima, H., et al *Nat. Chem. Biol.* **2007**, *3*, 576.
17. Kotake, Y.; Sagane, K.; Owa, T.; Mimori-Kiyosue, Y.; Shimizu, H.; Uesugi, M.; Ishihama, Y.; Iwata, M.; Mizui, Y. *Nat. Chem. Biol.* **2007**, *3*, 570.
18. Kamisuki, S.; Mao, Q.; Abu-Elheiga, L.; Gu, Z.; Kugimiya, A.; Kwon, Y.; Shinohara, T.; Kawazoe, Y.; Sato, S.; Asakura, K., et al *Chem. Biol.* **2009**, *16*, 882.

19. Choi, Y.; Kawazoe, Y.; Murakami, K.; Misawa, H.; Uesugi, M. *J. Biol. Chem.* **2003**, *278*, 7320.
20. Kahsai, A. W.; Zhu, S.; Wardrop, D. J.; Lane, W. S.; Fenteany, G. *Chem. Biol.* **2006**, *13*, 973.
21. Tsukita, S.; Hieda, Y. *J. Cell Biol.* **1989**, *108*, 2369.
22. Nakajima, H.; Sato, B.; Fujita, T.; Takase, S.; Terano, H.; Okuhara, M. *J. Antibiot. (Tokyo)* **1996**, *49*, 1196.
23. Nakajima, H.; Hori, Y.; Terano, H.; Okuhara, M.; Manda, T.; Matsumoto, S.; Shimomura, K. *J. Antibiot. (Tokyo)* **1996**, *49*, 1204.
24. Mizui, Y.; Sakai, T.; Iwata, M.; Uenaka, T.; Okamoto, K.; Shimizu, H.; Yamori, T.; Yoshimatsu, K.; Asada, M. *J. Antibiot. (Tokyo)* **2004**, *57*, 188.
25. Sakai, T.; Sameshima, T.; Matsufuji, M.; Kawamura, N.; Dobashi, K.; Mizui, Y. *J. Antibiot. (Tokyo)* **2004**, *57*, 173.
26. Sakai, T.; Asai, N.; Okuda, A.; Kawamura, N.; Mizui, Y. *J. Antibiot. (Tokyo)* **2004**, *57*, 180.
27. Chen, S.; Do, J. T.; Zhang, Q.; Yao, S.; Yan, F.; Peters, E. C.; Scholer, H. R.; Schultz, P. G.; Ding, S. *Proc. Natl. Acad. Sci. U.S.A.* **2006**, *103*, 17266.
28. Yang, J.; Shamji, A.; Matchacheep, S.; Schreiber, S. L. *Chem. Biol.* **2007**, *14*, 371.
29. Palacios, F.; Schweitzer, J. K.; Boshans, R. L.; D'Souza-Schorey, C. *Nat. Cell Biol.* **2002**, *4*, 929.
30. Jung, H. J.; Lee, H. B.; Kim, C. J.; Rho, J. R.; Shin, J.; Kwon, H. J. *J. Antibiot. (Tokyo)* **2003**, *56*, 492.
31. Jung, H. J.; Shim, J. S.; Lee, J.; Song, Y. M.; Park, K. C.; Choi, S. H.; Kim, N. D.; Yoon, J. H.; Mungai, P. T.; Schumacker, P. T., et al *J. Biol. Chem.* **2010**, *285*, 11584.
32. Suzuki, H.; Hosokawa, Y.; Toda, H.; Nishikimi, M.; Ozawa, T. *Biochem. Biophys. Res. Commun.* **1988**, *156*, 987.
33. Agard, N. J.; Prescher, J. A.; Bertozzi, C. R. *J. Am. Chem. Soc.* **2004**, *126*, 15046.
34. Rakic, B.; Clarke, J.; Tremblay, T. L.; Taylor, J.; Schreiber, K.; Nelson, K. M.; Abrams, S. R.; Pezacki, J. P. *Chem. Biol.* **2006**, *13*, 1051.
35. Hoffstrom, B. G.; Kaplan, A.; Letso, R.; Schmid, R. S.; Turmel, G. J.; Lo, D. C.; Stockwell, B. R. *Nat. Chem. Biol.* **2010**, *6*, 900.
36. Kanoh, N.; Kumashiro, S.; Simizu, S.; Kondoh, Y.; Hatakeyama, S.; Tashiro, H.; Osada, H. *Angew. Chem., Int. Ed.* **2003**, *42*, 5584.
37. Kawatani, M.; Okumura, H.; Honda, K.; Kanoh, N.; Muroi, M.; Dohmae, N.; Takami, M.; Kitagawa, M.; Futamura, Y.; Imoto, M., et al *Proc. Natl. Acad. Sci. U.S.A.* **2008**, *105*, 11691.
38. Sakamoto, S.; Kabe, Y.; Hatakeyama, M.; Yamaguchi, Y.; Handa, H. *Chem. Rec.* **2009**, *9*, 66.
39. Miller, M. T.; Stromland, K. *Teratology* **1999**, *60*, 306.
40. Melchert, M.; List, A. *Int. J. Biochem. Cell Biol.* **2007**, *39*, 1489.
41. Knobloch, J.; Ruther, U. *Cell Cycle* **2008**, *7*, 1121.
42. Ito, T.; Ando, H.; Suzuki, T.; Ogura, T.; Hotta, K.; Imamura, Y.; Yamaguchi, Y.; Handa, H. *Science* **2010**, *327*, 1345.
43. Higgins, J. J.; Pucilowska, J.; Lombardi, R. Q.; Rooney, J. P. *Neurology* **2004**, *63*, 1927.
44. Angers, S.; Li, T.; Yi, X.; MacCoss, M. J.; Moon, R. T.; Zheng, N. *Nature* **2006**, *443*, 590.
45. Groisman, R.; Polanowska, J.; Kuraoka, I.; Sawada, J.; Saijo, M.; Drapkin, R.; Kisselev, A. F.; Tanaka, K.; Nakatani, Y. *Cell* **2003**, *113*, 357.
46. Park, C.; Marqusee, S. *Nat. Methods* **2005**, *2*, 207.
47. Stankunas, K.; Bayle, J. H.; Gestwicki, J. E.; Lin, Y. M.; Wandless, T. J.; Crabtree, G. R. *Mol. Cell* **2003**, *12*, 1615.
48. Tucker, C. L.; Fields, S. *Nat. Biotechnol.* **2001**, *19*, 1042.
49. Lomenick, B.; Hao, R.; Jonai, N.; Chin, R. M.; Aghajan, M.; Warburton, S.; Wang, J.; Wu, R. P.; Gomez, F.; Loo, J. A., et al *Proc. Natl. Acad. Sci. U.S.A.* **2009**, *106*, 21984.
50. Wood, J. G.; Rogina, B.; Lavu, S.; Howitz, K.; Helfand, S. L.; Tatar, M.; Sinclair, D. *Nature* **2004**, *430*, 686.
51. Mezencev, R.; Kutschy, P.; Salayova, A.; Curillova, Z.; Mojzis, J.; Pilatova, M.; McDonald, J. *Chemotherapy* **2008**, *54*, 372.
52. Stefely, J. A.; Palchaudhuri, R.; Miller, P. A.; Peterson, R. J.; Moraski, G. C.; Hergenrother, P. J.; Miller, M. J. *J. Med. Chem.* **2010**, *53*, 3389.
53. Maurer, P. J.; Miller, M. J. *J. Am. Chem. Soc.* **1983**, *105*, 240.
54. Yaguchi, S.; Fukui, Y.; Koshimizu, I.; Yoshimi, H.; Matsuno, T.; Gouda, H.; Hirono, S.; Yamazaki, K.; Yamori, T. *J. Natl. Cancer Inst.* **2006**, *98*, 545.
55. Lamb, J.; Crawford, E. D.; Peck, D.; Modell, J. W.; Blat, I. C.; Wrobel, M. J.; Lerner, J.; Brunet, J. P.; Subramanian, A.; Ross, K. N., et al *Science* **2006**, *313*, 1929.
56. Wood, T. E.; Dalili, S.; Simpson, C. D.; Sukhai, M. A.; Hurren, R.; Anyiwe, K.; Mao, X.; Suarez Saiz, F.; Gronda, M.; Eberhard, Y., et al *Mol. Cancer Ther.* **2010**, *9*, 246.
57. Hieronymus, H.; Lamb, J.; Ross, K. N.; Peng, X. P.; Clement, C.; Rodina, A.; Nieto, M.; Du, J.; Stegmaier, K.; Raj, S. M., et al *Cancer Cell* **2006**, *10*, 321.
58. Muroi, M.; Kazami, S.; Noda, K.; Kondo, H.; Takayama, H.; Kawatani, M.; Usui, T.; Osada, H. *Chem. Biol.* **2010**, *17*, 460.
59. Kawatani, M.; Takayama, H.; Muroi, M.; Kimura, S.; Maekawa, T.; Osada, H. *Chem. Biol.* **2011**, *18*, 743.
60. Young, D. W.; Bender, A.; Hoyt, J.; McWhinnie, E.; Chirn, G. W.; Tao, C. Y.; Tallarico, J. A.; Labow, M.; Jenkins, J. L.; Mitchison, T. J., et al *Nat. Chem. Biol.* **2008**, *4*, 59.
61. Li, L.; Wang, H. K.; Kuo, S. C.; Wu, T. S.; Mauger, A.; Lin, C. M.; Hamel, E.; Lee, K. H. *J. Med. Chem.* **1994**, *37*, 3400.
62. Shi, Q.; Chen, K.; Morris-Natschke, S. L.; Lee, K. H. *Curr. Pharm. Des.* **1998**, *4*, 219.
63. Tong, Y. G.; Zhang, X. W.; Geng, M. Y.; Yue, J. M.; Xin, X. L.; Tian, F.; Shen, X.; Tong, L. J.; Li, M. H.; Zhang, C., et al *Mol. Pharmacol.* **2006**, *69*, 1226.
64. Sumiya, E.; Shimogawa, H.; Sasaki, H.; Tsutsumi, M.; Yoshita, K.; Ojika, M.; Suenaga, K.; Uesugi, M. *ACS Chem. Biol.* **2011**, *6*, 425.
65. Flanagan, M. D.; Lin, S. *J. Biol. Chem.* **1980**, *255*, 835.
66. Bai, R.; Covell, D. G.; Liu, C.; Ghosh, A. K.; Hamel, E. *J. Biol. Chem.* **2002**, *277*, 32165.
67. Bubb, M. R.; Senderowicz, A. M.; Sausville, E. A.; Duncan, K. L.; Korn, E. D. *J. Biol. Chem.* **1994**, *269*, 14869.
68. Coue, M.; Brenner, S. L.; Spector, I.; Korn, E. D. *FEBS Lett.* **1987**, *213*, 316.
69. Saito, S.; Watabe, S.; Ozaki, H.; Fusetani, N.; Karaki, H. *J. Biol. Chem.* **1994**, *269*, 29710.
70. Tanaka, C.; Tanaka, J.; Bolland, R. F.; Marriott, G.; Higa, T. *Tetrahedron* **2006**, 62.
71. Bubb, M. R.; Spector, I.; Bershadsky, A. D.; Korn, E. D. *J. Biol. Chem.* **1995**, *270*, 3463.
72. Ojika, M.; Inukai, Y.; Kito, Y.; Hirata, M.; Iizuka, T.; Fudou, R. *Chem. Asian J.* **2008**, *3*, 126.
73. Iizuka, T.; Fudou, R.; Jojima, Y.; Ogawa, S.; Yamanaka, S.; Inukai, Y.; Ojika, M. *J. Antibiot. (Tokyo)* **2006**, *59*, 385.
74. Teruya, T.; Sasaki, H.; Fukazawa, H.; Suenaga, K. *Org. Lett.* **2009**, *11*, 5062.
75. Gao, X.; Liu, Y.; Kwong, S.; Xu, Z.; Ye, T. *Org. Lett.* **2010**, *12*, 3018.
76. Soga, T.; Ohashi, Y.; Ueno, Y.; Naraoka, H.; Tomita, M.; Nishioka, T. *J. Proteome Res.* **2003**, *2*, 488.
77. Monton, M. R.; Soga, T. *J. Chromatogr., A* **2007**, *1168*, 237. discussion 236.
78. Hirayama, A.; Kami, K.; Sugimoto, M.; Sugawara, M.; Toki, N.; Onozuka, H.; Kinoshita, T.; Saito, N.; Ochiai, A.; Tomita, M., et al *Cancer Res.* **2009**, *69*, 4918.
79. Ishii, N.; Nakahigashi, K.; Baba, T.; Robert, M.; Soga, T.; Kanai, A.; Hirasawa, T.; Naba, M.; Hirai, K.; Hoque, A., et al *Science* **2007**, *316*, 593.
80. Soga, T.; Baran, R.; Suematsu, M.; Ueno, Y.; Ikeda, S.; Sakurakawa, T.; Kakazu, Y.; Ishikawa, T.; Robert, M.; Nishioka, T., et al *J. Biol. Chem.* **2006**, *281*, 16768.
81. Sugimoto, M.; Wong, D. T.; Hirayama, A.; Soga, T.; Tomita, M. *Metabolomics* **2010**, *6*, 78.
82. Faix, J.; Rottner, K. *Curr. Opin. Cell Biol.* **2006**, *18*, 18.
83. Mattila, P. K.; Lappalainen, P. *Nat. Rev. Mol. Cell Biol.* **2008**, *9*, 446.
84. Kitagawa, M.; Ikeda, S.; Tashiro, E.; Soga, T.; Imoto, M. *Chem. Biol.* **2010**, *17*, 989.
85. Parsons, A. B.; Brost, R. L.; Ding, H.; Li, Z.; Zhang, C.; Sheikh, B.; Brown, G. W.; Kane, P. M.; Hughes, T. R.; Boone, C. *Nat. Biotechnol.* **2004**, *22*, 62.
86. Parsons, A. B.; Lopez, A.; Givoni, I. E.; Williams, D. E.; Gray, C. A.; Porter, J.; Chua, G.; Sopko, R.; Brost, R. L.; Ho, C. H., et al *Cell* **2006**, *126*, 611.
87. Ayscough, K. R.; Stryker, J.; Pokala, N.; Sanders, M.; Crews, P.; Drubin, D. G. *J. Cell Biol.* **1997**, *137*, 399.
88. Torralba, S.; Raudaskoski, M.; Pedregosa, A. M.; Laborda, F. *Microbiology* **1998**, *144*, 45.
89. Yoshida, S.; Ikeda, E.; Uno, I.; Mitsuzawa, H. *Mol. Gen. Genet.* **1992**, *231*, 337.
90. Douglas, C. M.; Marrinan, J. A.; Li, W.; Kurtz, M. B. *J. Bacteriol.* **1994**, *176*, 5686.
91. Roe, S. M.; Prodromou, C.; O'Brien, R.; Ladbury, J. E.; Piper, P. W.; Pearl, L. H. *J. Med. Chem.* **1999**, *42*, 260.
92. Gupta, S. S.; Ton, V. K.; Beaudry, V.; Rulli, S.; Cunningham, K.; Rao, R. *J. Biol. Chem.* **2003**, *278*, 28831.
93. Kitagawa, I.; Kobayashi, M.; Imamoto, T.; Yasuzawa, T.; Kyogoku, Y. *Chem. Pharm. Bull.* **1981**, *29*, 2387.
94. Schmidt, E. W.; Bewley, C. A.; Faulkner, D. J. *J. Org. Chem.* **1998**, *63*, 1254.
95. Nishimura, S.; Arita, Y.; Honda, M.; Iwamoto, K.; Matsuyama, A.; Shirai, A.; Kawasaki, H.; Kakeya, H.; Kobayashi, T.; Matsunaga, S., et al *Nat. Chem. Biol.* **2010**, *6*, 519.
96. Matsunaga, S.; Fusetani, N. *J. Org. Chem.* **1995**, *60*, 1177.
97. Matsunaga, S.; Fusetani, N.; Hashimoto, K.; Walchli, M. *J. Am. Chem. Soc.* **1989**, *111*, 2582.
98. Wada, S.; Matsunaga, S.; Fusetani, N.; Watabe, S. *Mar. Biotechnol. (NY)* **2000**, *2*, 285.
99. Matsuyama, A.; Arai, R.; Yashiroda, Y.; Shirai, A.; Kamata, A.; Sekido, S.; Kobayashi, Y.; Hashimoto, A.; Hamamoto, M.; Hiraoka, Y., et al *Nat. Biotechnol.* **2006**, *24*, 841.
100. Shirai, A.; Matsuyama, A.; Yashiroda, Y.; Hashimoto, A.; Kawamura, Y.; Arai, R.; Komatsu, Y.; Horinouchi, S.; Yoshida, M. *J. Biol. Chem.* **2008**, *283*, 10745.

THE JOURNAL OF BIOLOGICAL CHEMISTRY VOL. 286, NO. 45, pp. 39259–39268, November 11, 2011

Involvement of 14-3-3 Proteins in the Second Epidermal Growth Factor-induced Wave of Rac1 Activation in the Process of Cell Migration*[S]

Received for publication, April 27, 2011, and in revised form, August 11, 2011 Published, JBC Papers in Press, August 25, 2011, DOI 10.1074/jbc.M111.255489

Hiroki Kobayashi[‡], Yusuke Ogura[§], Masato Sawada[‡], Ryoji Nakayama[‡], Kei Takano[‡], Yusuke Minato[‡], Yasushi Takemoto[‡], Etsu Tashiro[‡], Hidenori Watanabe[§], and Masaya Imoto[‡1]

From the [‡]Department of Biosciences and Informatics, Faculty of Science and Technology, Keio University, 3-14-1 Hiyoshi, Kohoku-ku, Yokohama 223-8522, Japan and the [§]Graduate School of Agricultural and Life Sciences, The University of Tokyo, 1-1-1 Yayoi, Bunkyo-ku, Tokyo 113-8657, Japan

Background: The spatiotemporal regulation of Rac1 controls cell migration.
Results: EGF induced two waves of Rac1 activation in the process of cell migration.
Conclusion: 14-3-3 proteins regulate the second EGF-induced wave of Rac1 activation by interacting with RacGEF.
Significance: The second wave of Rac1 activation might be required for EGF-induced cell migration.

Immense previous efforts have elucidated the core machinery in cell migration, actin remodeling regulated by Rho family small GTPases including RhoA, Cdc42, and Rac1; however, the spatiotemporal regulation of these molecules remains largely unknown. Here, we report that EGF induces biphasic Rac1 activation in the process of cell migration, and UTKO1, a cell migration inhibitor, inhibits the second EGF-induced wave of Rac1 activation but not the first wave. To address the regulation mechanism and role of the second wave of Rac1 activation, we identified 14-3-3ζ as a target protein of UTKO1 and also showed that UTKO1 abrogated the binding of 14-3-3ζ to Tiam1 that was responsible for the second wave of Rac1 activation, suggesting that the interaction of 14-3-3ζ with Tiam1 is involved in this event. To our knowledge, this is the first report to use a chemical genetic approach to demonstrate the mechanism of temporal activation of Rac1.

The importance of cell migration is evident from the number of physiological processes that depend on the regulated movement of cells, including embryonic development, immune responses, and tissue maintenance and repair, and also from the disease states driven by aberrant cell motility, such as chronic inflammation, vascular disease, and tumor metastasis (1). Key to the capacity of the cell to migrate is dynamic reorganization of the actin cytoskeleton (2). When a cell moves, site-directed *de novo* nucleation and polymerization of actin drives protrusive membrane structures such as lamellipodia and filopodia, which generate the locomotive force in migrating cells (3, 4). Reorganization of the actin cytoskeleton is regulated by actin-nucleating factors, the most prominent of which is the Arp2/3 complex (5). Catalytic activation of this complex is mediated by WASP/WAVE family members, which in turn translate extracellular signals via the Rho family of small GTPases such as RhoA, Cdc42, and Rac1 (6). In particular, activation of RhoA increases cell contractility and leads to the formation of focal adhesions and stress fibers (7). Activation of Cdc42 and Rac1 propagates the formation of filopodia and lamellipodia, respectively (8, 9).

The Rho family GTPases function as binary switches that cycle between an active GTP-bound form and an inactive GDP-bound form. This cycling is regulated through three factors: guanine nucleotide exchange factor (GEF),[2] GTPase-activating protein, and guanine nucleotide dissociation inhibitor (10, 11). Among them, GEF activates the Rho family GTPases by promoting the exchange of GDP with GTP, resulting in the binding of the GTPases to their effectors. A number of GEFs have been shown to transduce signals from many growth factors to the Rho family GTPases. In addition to the increasing number of GEFs, the redundant specificity of GEFs renders signaling networks controlling cell migration difficult to understand; many GEFs have been shown to take multiple Rho family GTPases as substrates, at least *in vitro* (11, 12). The spatiotemporal coordination of the Rho family GTPases by these molecules regulates a complicated dynamic process of cell migration.

Inhibitors of cell migration would be useful not only as tools for basic research into cell migration but also as anti-metastatic drug-leads for cancer therapy. To obtain cell migration inhibitor, UTKO1 was synthesized as a derivative of natural products moverastins, which inhibit migration of EC17 cells by inhibiting farnesylation of H-Ras (13). However, although its chemical structure is very similar to that of moverastins, its inhibitory effect on cell migration was stronger than that of the moverastins and did not involve inhibition of farnesyltransferase (14). UTKO1 also failed to inhibit MEK/ERK and the PI3K/Akt path-

* This work was supported by a grant from the Ministry of Education, Culture, Sports, Science, and Technology.
[S] The on-line version of this article (available at http://www.jbc.org) contains supplemental text, Scheme S1, and Figs. S1–S9.
[1] To whom correspondence should be addressed: Dept. of Biosciences and Informatics, Faculty of Science and Technology, Keio University, 3-14-1 Hiyoshi, Kohoku-ku, Yokohama 223-8522, Japan. Tel./Fax: 81-45-566-1557; E-mail: imoto@bio.keio.ac.jp.

[2] The abbreviations used are: GEF, guanine nucleotide exchange factor; IP, immunoprecipitation; CBB, Coomassie Brilliant Blue; EGF, epidermal growth factor.

way generally known to regulate cell migration.[3] This unique pharmacological profile of UTKO1 has drawn considerable interest, prompting us to further investigate its mechanism of action. In this report, we present evidence that EGF induces two waves of Rac1 activation in the process of cell migration and that UTKO1 inhibited only the second of these waves by targeting 14-3-3ζ. Furthermore, we showed that UTKO1 abrogated the binding of 14-3-3ζ to Tiam1 that was responsible for the second wave of Rac1 activation, presumably resulting in the inhibition of EGF-induced cell migration.

EXPERIMENTAL PROCEDURES

DNA Constructs—Human cDNA for 14-3-3s (α/β, ε, η, γ, τ/θ, ζ/δ, and σ) were amplified from HeLa cell cDNA and cloned into pcDNA3 (Invitrogen, San Diego, CA) with the N-terminal FLAG tag. All of the constructs were cloned into pGEX-2T (GE Healthcare, Princeton, NJ) to prepare GST fusion proteins in bacteria. Expression vectors encoding GST-fused 14-3-3ζ mutants (ΔC100, 1–145 amino acids; ΔC200, 1–45 amino acids; and C50, 196–245 amino acids) were generated by PCR using pGEX-2T/14-3-3ζ as a template. pCS2+MT/Tiam1, a expression vector encoding human Tiam1 followed by 6×Myc, was kindly provided by Dr. H. Sugimura (Hamamatsu University School of Medicine, Hamamatsu, Japan).

Chemotaxis Chamber Assay—Cell migration was assayed with a chemotaxis chamber (Becton Dickinson, Franklin Lakes, NJ). A431 cells suspended in DMEM supplemented with 0.2% calf serum were incubated in the upper chamber; the lower chamber contained DMEM supplemented with 0.2% calf serum in the presence or absence of EGF (30 ng/ml). Drugs were added to both chambers. Following 24 h of incubation, the filter was fixed with MeOH and stained with hematoxylin (Sigma, St. Louis, MO). The cells attached to the lower side of the filter were counted.

Confocal Laser Scanning Microscopy—Cells were fixed with 3% paraformaldehyde for 15 min and permeabilized with 0.5% Triton X-100 in PBS for 5 min. After rinsing three times with PBS, the cells were incubated in blocking buffer (1% bovine serum albumin in PBS) for 30 min then stained with Texas Red®-X phalloidin (1:100; Molecular Probes, Eugene, OR) at room temperature for 1 h. Fluorescence images were obtained using a confocal laser scanning microscope system FV1000 (Olympus, Tokyo, Japan). Lamellipodia formation (%) means the ratio of the number of cells with lamellipodia in the total cell count.

Detection of Active Rac1—The cells were lysed with magnesium-containing lysis buffer (25 mM HEPES, pH 7.5, 150 mM NaCl, 1% Nonidet P-40, 0.25% sodium deoxycholate, 10% glycerol, 25 mM NaF, 10 mM $MgCl_2$, 1 mM EDTA, 1 mM Na_3VO_4, and a protease inhibitor mixture (Roche Applied Science)). The cell lysates were cleared by centrifugation at 15,000 × *g* for 10 min at 4 °C. Pak1 PBD-agarose (Millipore, Bedford, MA) was incubated with the lysates at 4 °C for 1 h and washed three times with magnesium-containing lysis buffer, and then active Rac1 was eluted by boiling in SDS sample buffer for 5 min. The resultant samples were subjected to Western blotting.

Identification of B-UTKO1 Binding Proteins—A431 cells were stimulated with EGF (30 ng/ml) for 4 h. The cells were collected and sonicated twice in immunoprecipitation (IP) buffer (50 mM HEPES, pH 7.5, 150 mM NaCl, 2.5 mM EGTA, 1 mM EDTA, 1 mM DTT, and a protease inhibitor mixture) for 10 s. The cell lysates were centrifuged at 130,000 × *g* for 1 h at 4 °C. The resulting supernatant was precleared twice with avidin beads (Pierce) for 1 h and incubated with biotin (50 nmol) or B-UTKO1ox (50 nmol) and avidin beads at 4 °C overnight. The beads were washed three times with IP buffer and once with PBS. The bound proteins were eluted with 2 mM biotin in PBS and concentrated by a centrifugal filter device (Ultracel (YM-10); Millipore). The resulting proteins were subjected to SDS-PAGE followed by Coomassie Brilliant Blue (CBB) staining (see Fig. 3*B*) or immunoblotting (see Fig. 4*A*). Following CBB staining, the bands corresponding to the UTKO1 binding proteins were excised, and the gel pieces were destained with 50% CH_3CN in 50 mM NH_4HCO_3 solution. After removal of the supernatant, cysteine residues were reduced with DTT, carbamidomethylated with indoacetamide, and the proteins were digested with trypsin at 37 °C overnight. The tryptic peptides were recovered by sequentially adding three solvent systems containing 50% CH_3CN and 1% TFA; 20% HCOOH, 25% CH_3CN and 15% *i*-PrOH; and 80% CH_3CN. The supernatants were collected and pooled into one tube, reducing the volume *in vacuo*. The dried tryptic peptides were suspended in 2% CH_3CN and 0.1% TFA and applied to the following LC-MS/MS system. Chromatographic separation was accomplished with the MAGIC 2002 HPLC system (Michrom BioResources). Peptide samples were loaded onto a Cadenza C18 custom-packed column (0.2 × 50 mm; Michrom BioResources) and eluted using a linear gradient of 5–60% CH_3CN in 0.1% HCOOH for 30 min at a flow rate of 1 ml/min. Samples were ionized with a Nanoflow-LC ESI, and MS/MS spectrum data were obtained with an LCQ-Deca XP ion trap mass spectrometer (Thermo Electron). The Mascot data base searching software (Matrix Science) was used for the identification of B-UTKO1ox binding proteins.

Immunoprecipitation—A431/FLAG-14-3-3ζ cells were transiently transfected with pCS2+MT/Tiam1 using Metafectene Pro (Biontex, Munich, Germany). Following 24 h of transfection, the cells were pretreated with UTKO1 for 15 min and stimulated with EGF for 12 h. The cells were collected and sonicated in IP buffer. The cell lysates were cleared by centrifugation at 15,000 × *g* for 15 min at 4 °C then incubated with anti-FLAG antibody and protein A/G-agarose beads (Santa Cruz, Santa Cruz, CA) at 4 °C overnight. The immunoprecipitants were washed once with IP buffer and twice with IP buffer containing 1% Nonidet P-40. The bound proteins were eluted by boiling in SDS sample buffer for 5 min and subjected to Western blotting.

In Vitro B-UTKO1 Pulldown Assay—GST fusion proteins, which were expressed in the *Escherichia coli* DH5α strain and purified using glutathione-Sepharose 4B (GE Healthcare), were incubated with B-UTKO1ox and avidin beads in 500 μl of IP

[3] S. Magi and M. Imoto, unpublished observations.

buffer for 3 h. The beads were washed and eluted with 2 mM biotin in PBS. The eluted proteins were subjected to SDS-PAGE. For the competition assay, UTKO1 was added before incubating with B-UTKO1ox.

GST Pulldown Assay—The collected cells were sonicated twice in IP buffer for 10 s. The cell lysates were cleared by centrifugation at 15,000 × *g* for 15 min at 4 °C and then incubated with purified GST or GST-14-3-3ζ and glutathione-Sepharose 4B (GE Healthcare) for 2 h. The bound proteins were eluted by boiling in SDS sample buffer for 5 min and subjected to Western blotting. For Fig. 6*A*, purified GST-14-3-3ζ was preincubated with UTKO1 in a total volume of 1 ml of IP buffer for 1 h. Other experimental procedures are given in the supplemental materials.

RESULTS

UTKO1 Inhibits the Second EGF-induced Wave of Lamellipodia Formation—The formation of lamellipodia, protruding membrane structures at the leading edge of migrating cells, is key in cell migration (15). We observed transient lamellipodia formation at 5 min following EGF stimulation, as reported elsewhere (12, 16), and we also found a second wave of lamellipodia formation to be initiated at 6–9 h and reach its zenith within 12 h after EGF stimulation in human epidermoid carcinoma A431 cells (Fig. 1, *A* and *B*). Furthermore, we found that UTKO1 (Fig. 1*C*), a cell migration inhibitor (14), inhibited only the second wave of that as shown in Fig. 1 (*D–G*); we evaluated the effect of UTKO1 on the lamellipodia formation induced by treatment with EGF for 5 min and for 12 h, respectively, and found no inhibition of lamellipodia formation at 5 min; lamellipodia formation at 12 h was inhibited by UTKO1 with an IC_{50} value of 0.78 μM. This IC_{50} value is almost the same as that for inhibiting cell migration (0.67 μM; Fig. 1*H*). Similar results were obtained when TT cells, a human esophageal cancer cell line, were used in place of A431 cells (supplemental Fig. S1). Thus, although EGF induced two waves of lamellipodia formation, at 5 min and 12 h after stimulation, UTKO1 inhibited only the second wave.

UTKO1 Inhibits the Second EGF-induced Wave of Rac1 Activation—Lamellipodia formation has been reported to be mainly regulated by Rac1, a member of the Rho family of small GTPases (9, 17). Because lamellipodia formation was observed at 5 min and 12 h following EGF stimulation, we next examined whether EGF also induces two waves of Rac1 activation. Rac1 was rapidly and transiently activated at 2–5 min after EGF stimulation, as expected from previous published reports (12, 18), and we also found that active Rac1 began to increase from 6 h onward. This second wave of Rac1 activation was much broader than the first wave and lasted until 12 h after EGF stimulation (Fig. 2*A*). UTKO1 did not inhibit the first wave of Rac1 activation even when the cells were pretreated with UTKO1 for 12 h but did inhibit the second wave (Fig. 2, *B* and *C*). Similar results were obtained when TT cells were used in place of A431 cells (supplemental Fig. S2). Moreover, when UTKO1 was added at 4 h after EGF stimulation, the second EGF-induced wave of Rac1 activation, lamellipodia formation, and cell migration were all inhibited (Fig. 2, *D–F*). These results indicate that UTKO1 suppresses EGF-induced cell migration, possibly via inhibition of the second wave of Rac1 activation required for lamellipodia formation.

Identification of 14-3-3ζ as a UTKO1-binding Protein—To elucidate the mechanism for the inhibition of cell migration caused by UTKO1, we tried to identify the target protein of UTKO1 responsible for Rac1 activation at 12 h following EGF stimulation. We used biotinylated UTKO1s (B-UTKO1ox and B-UTKO1ph) (Fig. 3*A* and supplemental Scheme S1), which were biologically active with the same potency as UTKO1. Lysates of A431 cells stimulated with EGF for 4 h were incubated overnight with B-UTKO1ox and avidin beads. The B-UTKO1ox-bound avidin beads were precipitated and washed, and co-precipitated proteins were eluted by excess biotin. The eluted proteins were separated by SDS-PAGE and detected by CBB staining (Fig. 3*B*). We observed 10 major protein bands that specifically co-precipitated with B-UTKO1oxand identified these proteins by LC-MS/MS system as: 1) GRP78; 2) PDI; 3) nucleobindin-2; 4) 2-phosphopruvate-hydratase α-enolase; 5) unnamed product; 6) unnamed product; 7) mutant β-actin; 8) annexin A2; 9) 14-3-3ϵ; and 10) 14-3-3ζ. The peptide sequences of unnamed products 5 and 6 suggest them to be nuclear lamin proteins. Of these 10 proteins, we speculated that 14-3-3ζ might be the target of UTKO1, because it has been previously reported to relate to the formation of lamellipodia (19, 20). The binding of UTKO1 to 14-3-3ζ was confirmed by Western blotting of B-UTKO1ox- or B-UTKO1ph-bound proteins using anti-14-3-3ζ antibody, as shown in Fig. 4*A*. Next, to determine whether UTKO1 could bind directly to 14-3-3ζ, we performed *in vitro* B-UTKO1 pulldown experiments using purified GST-tagged 14-3-3ζ. GST-14-3-3ζ co-precipitated with B-UTKO1ox: competition was clearly observed in the presence of UTKO1 (Fig. 4*B*). These results suggest that UTKO1 binds directly to 14-3-3ζ. Moreover, we found that B-UTKO1ox did not bind to a C terminus deletion mutant of 14-3-3ζ, indicating that the binding of UTKO1 to 14-3-3ζ is probably via the C-terminal region (supplemental Fig. S3). 14-3-3ζ is a member of the 14-3-3 family, and at least seven different isoforms have been identified in mammalian cells (21, 22). Therefore, we prepared seven recombinant GST-14-3-3 isoforms and performed *in vitro* B-UTKO1 pulldown experiments to test each for its ability to bind to UTKO1. As a result, the ζ isoform showed the strongest binding ability to B-UTKO1ox (Fig. 4*C*).

Next, we performed RNAi experiments to investigate whether the loss of 14-3-3ζ could suppress EGF-induced cell migration, lamellipodia formation, and Rac1 activation in A431 cells. The successful knockdown of 14-3-3ζ by siRNA was confirmed by Western blotting (Fig. 4*D*). Silencing of 14-3-3ζ expression consequently suppressed EGF-induced cell migration in A431 cells (Fig. 4*E*). Furthermore, silencing of 14-3-3ζ expression did not inhibit EGF-induced Rac1 activation at 2 min and lamellipodia formation at 5 min but did inhibit both EGF-induced Rac1 activation and lamellipodia formation at 12 h, as shown in Fig. 4 (*F–H*). These results indicate that 14-3-3ζ acts upstream of the second EGF-induced wave of Rac1 activation. Additionally, EGF-induced filopodia-like structures observed in 14-3-3ζ knockdown A431 cells (Fig.

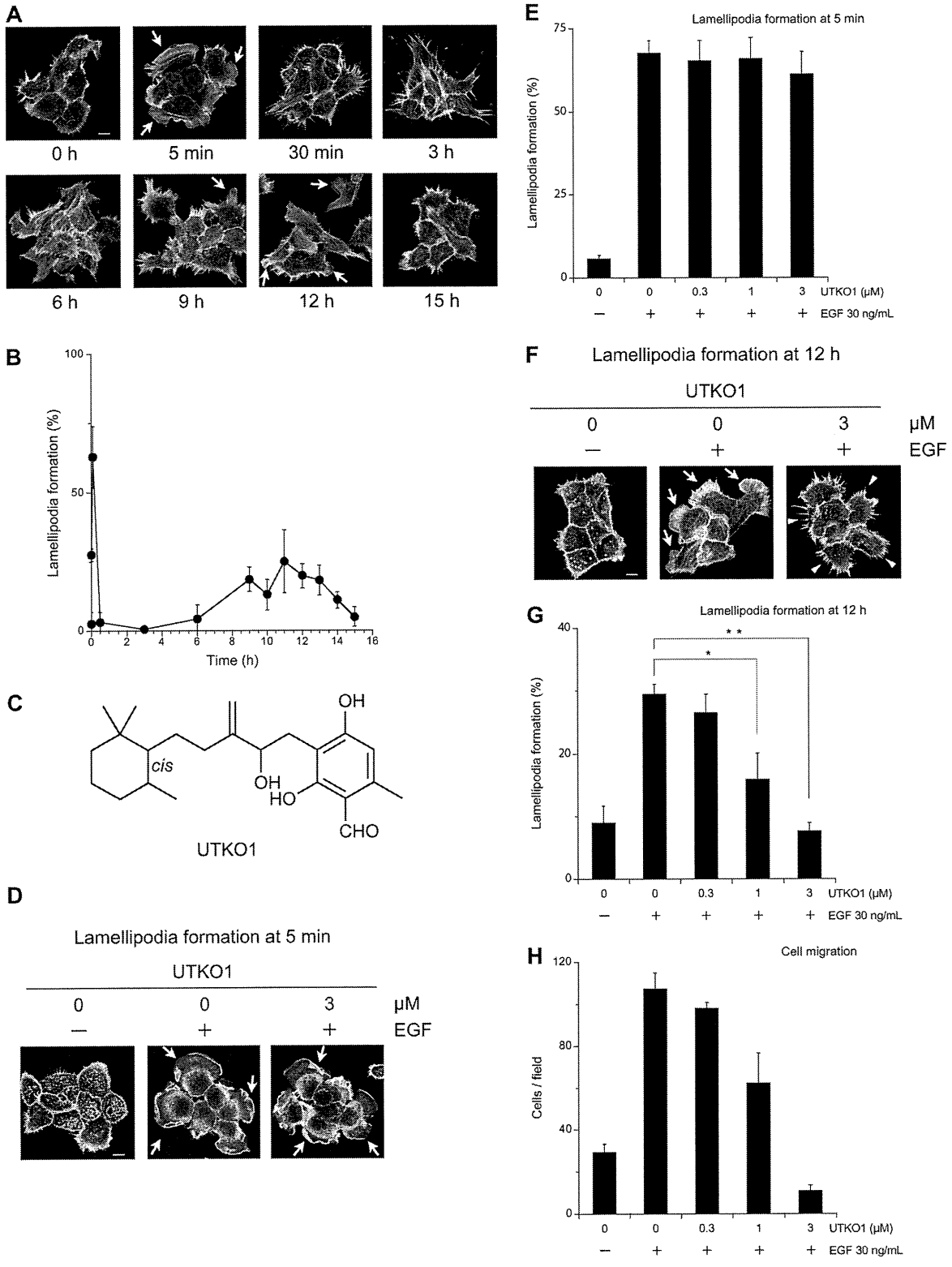

FIGURE 1. **UTKO1 inhibits the second EGF-induced wave of lamellipodia formation in A431 cells.** *A* and *B*, EGF-induced lamellipodia formation in A431 cells, observed under confocal microscopy (*A*) and counted (*B*). *C*, structure of UTKO1. *D–G*, effect of UTKO1 on EGF-induced lamellipodia formation. A431 cells were pretreated with the indicated concentrations of UTKO1 for 15 min and stimulated with EGF. After 5 min (*D* and *E*) or 12 h (*F* and *G*), the cells were observed under confocal microscopy (*D* and *F*) and counted (*E* and *G*). The data represent the means ± S.D. ($n = 6$). *H*, inhibitory activity of UTKO1 on EGF-induced cell migration, monitored using a chemotaxis chamber. The data represent the means ± S.D. ($n = 5$). Throughout, the data were representative of at least three independent studies. *Arrows*, lamellipodia; *arrowheads*, see text. *Scale bar*, 10 μm. For *G*, statistical analyses were performed with a two-tailed Student's *t* test. *, $p = 0.00013$; **, $p = 1.0 \times 10^{-5}$. For *B*, *E*, and *G*, more than 300 cells were analyzed per experiment.

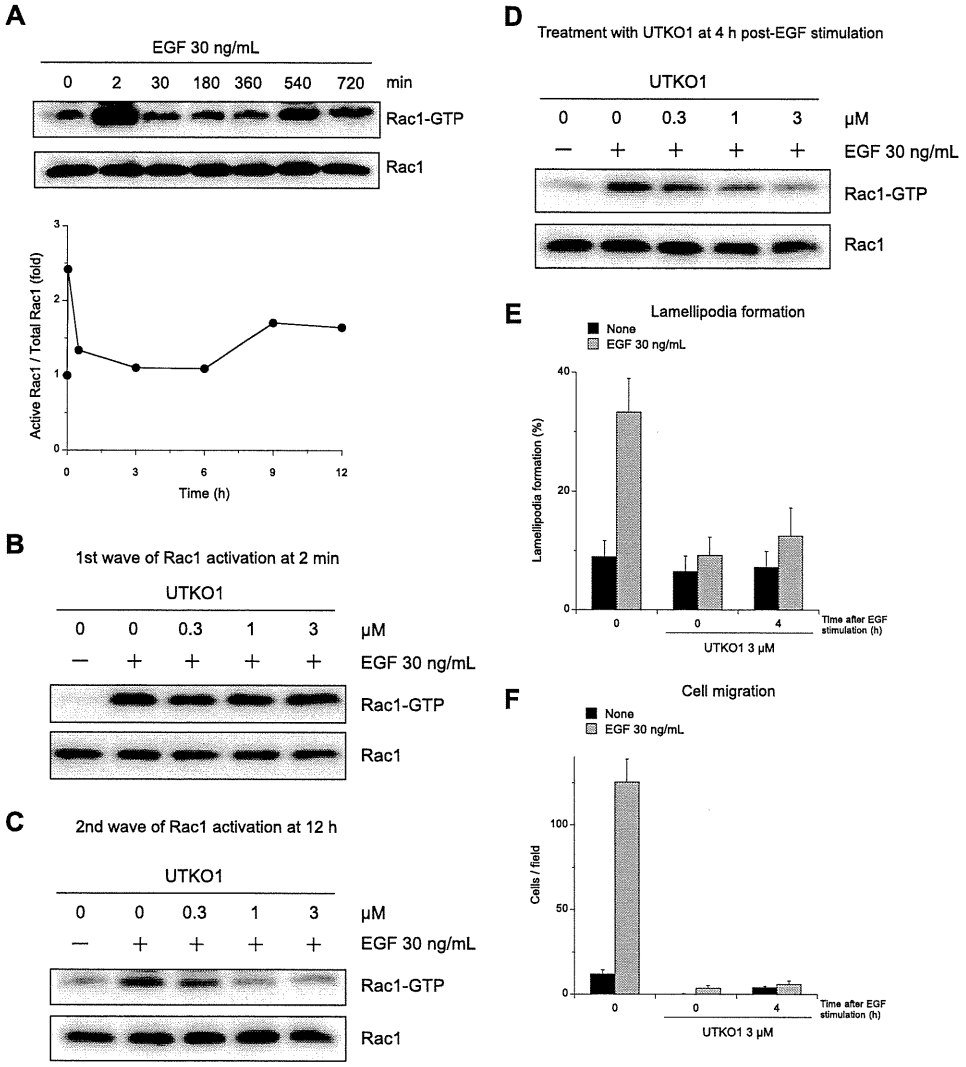

FIGURE 2. **UTKO1 inhibits the second EGF-induced wave of Rac1 activation in A431 cells.** *A*, time course analysis of Rac1 activation following EGF stimulation. A431 cells were stimulated with EGF for the indicated periods, and then the cells were examined for active Rac1 by pulldown assay (*upper panel*); signal intensities of Rac1-GTP were quantified, normalized to total Rac1 expression, using Image J software (National Institutes of Health, *lower panel*). *B* and *C*, effect of UTKO1 on EGF-induced Rac1 activation. A431 cells were pretreated with UTKO1 for 12 h (*B*) or 15 min (*C*) and stimulated with EGF. Following 2 min (*B*) or 12 h (*C*) of incubation, the cells were examined for active Rac1 by pulldown assay. *D–F*, UTKO1 inhibits only the second wave of Rac1 activation. A431 cells were stimulated with EGF for 4 h, and then the cells were treated with 3 μM UTKO1. After a further 8 h of incubation, the cells were examined for active Rac1 by pulldown assay (*D*), or the cells with lamellipodia were counted (*E*). The data represent the means ± S.D. ($n = 6$). *F*, A431 cells were incubated in the upper chamber and stimulated with EGF. Following 4 h of incubation, the cells were treated with UTKO1. After a further 20 h of incubation, the migrated cells were counted. The data represent the means ± S.D. ($n = 5$). Throughout, the data were representative of at least three independent studies. For *E*, more than 300 cells were analyzed per experiment.

4*G*, *arrowheads*) are similar to those observed in UTKO1-treated A431 cells stimulated with EGF (Fig. 1*F*, *arrowheads*). These filopodia-like structures might be formed as the result of a failure in the formation of a branched actin network as observed in a previously reported case (23). These observations also support the conclusion that the functional defect in 14-3-3ζ was induced by the treatment of cells with UTKO1. Furthermore, we showed that UTKO1 did not affect the expression levels of 14-3-3ζ (Fig. 4*I*). Taken together, these results suggest that UTKO1 binds to and inactivates 14-3-3ζ, resulting in inhibition of the second EGF-induced wave of Rac1 activation and subsequent suppression of lamellipodia formation and cell migration.

UTKO1 Inhibits the Interaction between 14-3-3ζ and Tiam1—Next, we examined the mechanism underlying the inhibition of Rac1 activation caused by the binding of UTKO1 to 14-3-3ζ. First, we examined the role of 14-3-3ζ in EGF-induced Rac1 activation. Because 14-3-3 proteins act as adaptor or "chaperone molecules" and interact with various cellular proteins (24), we hypothesized that a binding partner of 14-3-3ζ would regulate the second EGF-induced wave of Rac1 activation, and the most likely candidate binding partner is RacGEF. Thus, we investigated RacGEFs to see which would interact with 14-3-3ζ at 12 h following EGF stimulation by pulldown experiments using GST-14-3-3ζ. As shown in Fig. 5*A*, we verified that 14-3-3ζ interacts with both Tiam1 and βPix, as described in previous reports (19, 25, 26). We subsequently performed RNAi experiments to examine whether these GEFs are actually responsible for the second EGF-induced wave of Rac1 activation. As shown in Fig. 5*B*,

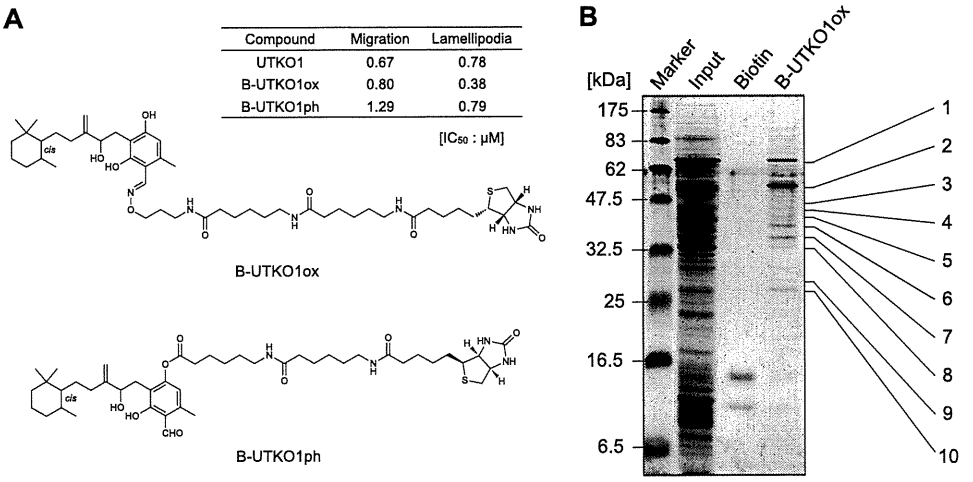

FIGURE 3. **Identification of UTKO1 binding proteins.** *A*, structures and bioactivities of B-UTKO1s. Bioactivities are shown as IC_{50} values in chemotaxis chamber assay and in lamellipodia formation assay. *B*, purification of UTKO1 binding proteins. Lysates of A431 cells stimulated with EGF for 4 h were incubated with biotin (50 nmol) or B-UTKO1ox (50 nmol) and avidin beads overnight. The beads were washed, and co-precipitated proteins were eluted with 2 mM biotin. The eluted proteins were subjected to SDS-PAGE followed by CBB staining. The co-precipitated proteins for B-UTKO1ox were identified as described under "Experimental Procedures."

silencing of Tiam1 expression suppressed in part (50% suppression) the second EGF-induced wave of Rac1 activation, whereas silencing of βPix expression had almost no effect. Furthermore, knockdown of Tiam1 suppressed both the second EGF-induced wave of lamellipodia formation and cell migration (Fig. 5, *C* and *D*). We also showed that Tiam1 is not involved in the first wave of Rac1 activation (supplemental Fig. S4). Similar results were obtained when TT cells were used in place of A431 cells (supplemental Fig. S5). These results demonstrate that Tiam1 is involved in the process of EGF-induced cell migration and therefore might function as the RacGEF responsible for the second EGF-induced wave of Rac1 activation by interacting with 14-3-3ζ.

Because UTKO1 binds to 14-3-3ζ and inhibits Rac1 activation, we examined the possibility that binding of UTKO1 to 14-3-3ζ abrogates the interaction between 14-3-3ζ and Tiam1. Lysates of A431 cells stimulated with EGF for 12 h were incubated with GST-14-3-3ζ in the presence or absence of UTKO1, and Tiam1 that co-precipitated with glutathione-Sepharose 4B was detected by Western blotting using anti-Tiam1 antibody. As shown in Fig. 6*A*, UTKO1 reduced the amount of 14-3-3ζ-bound Tiam1, indicating that it inhibited the interaction between 14-3-3ζ and Tiam1. Inhibition of the interaction between 14-3-3ζ and its binding partner by UTKO1 is not non-specific, because UTKO1 also inhibited the interaction between 14-3-3ζ and βPix but did not affect the interaction between 14-3-3ζ and kinesin. Subsequently, we confirmed the inhibition of the interaction between 14-3-3ζ and Tiam1 by UTKO1 in cultured cells by immunoprecipitation assay. A431 cells stably expressing FLAG-14-3-3ζ (A431/FLAG-14-3-3ζ cells) transiently transfected with Tiam1–6×Myc were stimulated with EGF for 12 h in the presence or absence of UTKO1. The cells were lysed, and the protein complexes that were precipitated with anti-FLAG antibody were detected by Western blotting. As shown in Fig. 6*B*, the amount of Tiam1 bound to FLAG-14-3-3ζ was reduced in a dose-dependent manner following treatment with UTKO1, confirming that UTKO1 directly inhibits the interaction between 14-3-3ζ and Tiam1 through binding to 14-3-3ζ.

DISCUSSION

Exposure of cells to growth factors leads to a variety of cellular responses at different times after stimulation. Some signaling molecules responsible for growth factor-stimulated cellular responses are activated by exposure to growth factor not only acutely, but also at a later time. For example, platelet-derived growth factor activates PI3K and PKC within minutes of stimulation and then again after 3–7 and 5–9 h, respectively (27). In addition, it has been reported that there are two distinct times during G_1 phase when Ras activity is needed for cell cycle progression (28). Moreover, in endothelial cells, biphasic activation of Rac1 has been reported, with the first peak between 1 and 2 h and the second peak at 8 h after induction by wound scratch/IL-1β (29).

We found that EGF induced distinct waves of Rac1 activation. When A431 cells are stimulated with EGF, Rac1 activation begins to wane after 5–20 min as previously reported (12, 16, 18); we also detected a second, prolonged wave of Rac1 activation 6–12 h after EGF stimulation (Fig. 2*A*). The regulation mechanism and role of early EGF-induced Rac1 activation have been extensively studied (12, 18, 30), but the second wave of Rac1 activation has not yet been examined.

UTKO1, an inhibitor of cell migration, was found to inhibit the second EGF-induced wave of Rac1 activation, but not the first wave (Fig. 2, *B–F*). Therefore, UTKO1 provides a useful chemical probe for the elucidation of the regulation mechanism and role of the second wave of Rac1 activation in cell migration. Our first step was to identify the molecular target of UTKO1 as 14-3-3ζ. This conclusion is supported by the following findings: 1) 14-3-3ζ was detected in affinity-purified proteins with biotin-conjugated UTKO1 prepared from lysates of A431 cells stimulated with EGF for 4 h (Figs. 3*B* and 4*A*); 2) biotin-conjugated UTKO1 bound directly to recombinant 14-3-3ζ (Fig. 4*B*); 3) knockdown of 14-3-3ζ by

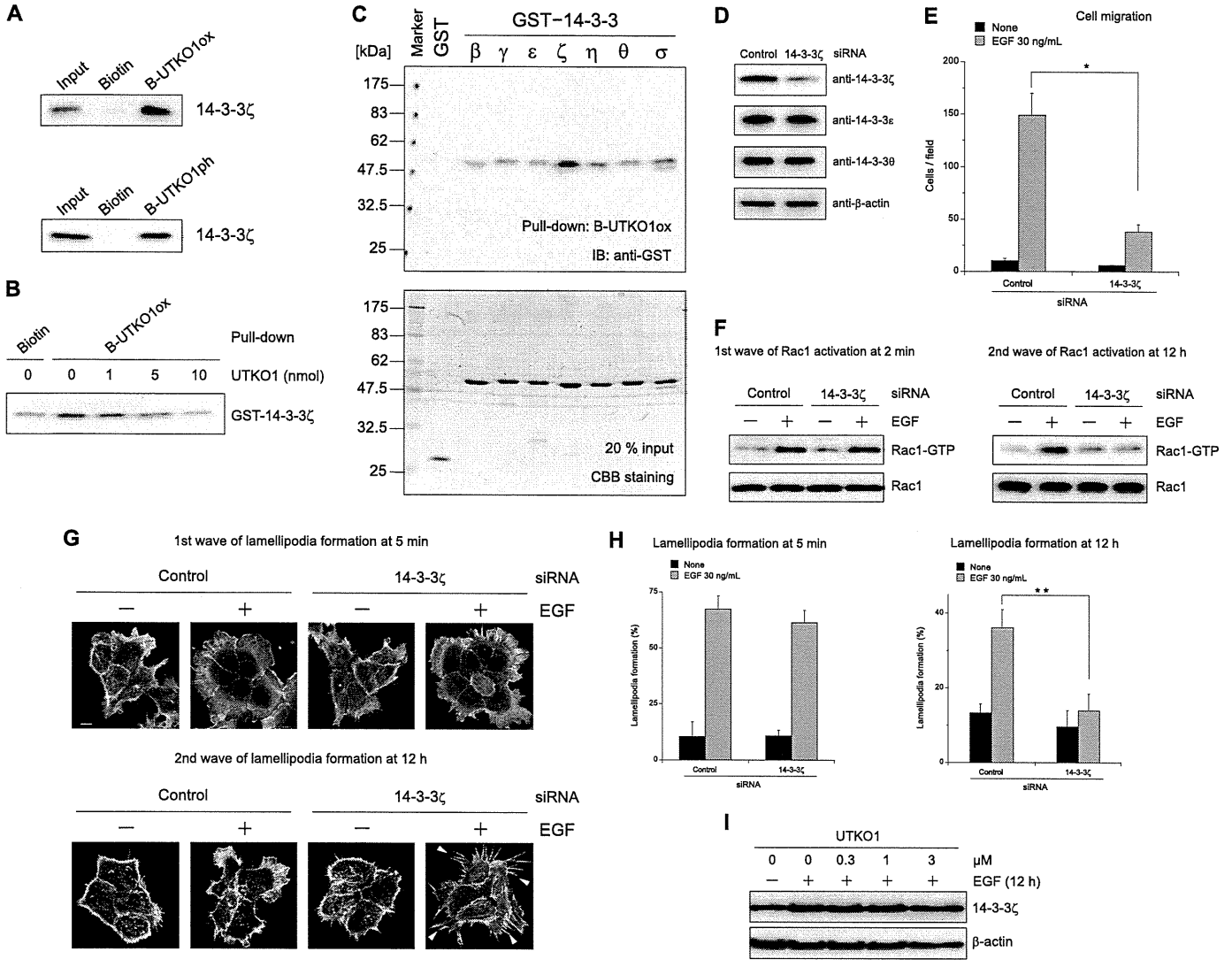

FIGURE 4. **Identification of 14-3-3ζ as a target protein of UTKO1.** *A*, confirmation of the binding of UTKO1 to 14-3-3ζ with Western blotting using anti-14-3-3ζ antibody. *B*, competition assay. Purified GST-tagged 14-3-3ζ (2.5 μg) was preincubated with UTKO1 as a competitor and was treated with biotin (0.5 nmol) or B-UTKO1ox (0.5 nmol) and avidin beads. The precipitated proteins were subjected to Western blotting using anti-GST antibody. *C*, determination of the binding ability of 14-3-3 isoforms to UTKO1. Purified GST or GST-tagged 14-3-3 isoforms were incubated with B-UTKO1ox and avidin beads. The precipitated proteins were subjected to Western blotting using anti-GST antibody (*upper panel*). GST or GST-tagged proteins used for the assay were subjected to SDS-PAGE followed by CBB staining as 20% input (*lower panel*). *D–H*, knockdown experiments. *D*, A431 cells were transfected with control or 14-3-3ζ siRNA and cultured for 72 h. Then the cells were collected and subjected to Western blotting using the indicated antibodies. *E*, control or 14-3-3ζ siRNA-transfected A431 cells were incubated in the upper chamber and stimulated with or without EGF for 24 h, and then the migrated cells were counted. The data represent the means ± S.D. ($n = 5$). *F–H*, control or 14-3-3ζ siRNA-transfected A431 cells were stimulated with EGF for 2 min or 12 h. Then the cells were examined for active Rac1 by pulldown assay (*F*), or the cells were observed under confocal microscopy (*G*), and counted (*H*). *Arrowheads* in *G*, see text. *Scale bar*, 10 μm. The data represent the means ± S.D. ($n = 6$). *I*, effect of UTKO1 on expression levels of 14-3-3ζ protein. A431 cells were pretreated with UTKO1 for 15 min and stimulated with EGF for 12 h. Then the cells were collected and subjected to Western blotting using the indicated antibodies. For *E* and *H*, statistical analyses were performed with a two-tailed Student's *t* test. *, $p = 9.3 \times 10^{-6}$; **, $p = 3.3 \times 10^{-7}$. Throughout, the data were representative of at least three independent studies. For *H*, more than 300 cells were analyzed per experiment. *IB*, immunoblot.

siRNA inhibited the second EGF-induced wave of Rac1 activation but not the first wave (Fig. 4*F*); and 4) the morphology of 14-3-3ζ-deficient A431 cells was very similar to that of UTKO1-treated A431 cells (Figs. 1*F* and 4*G*).

14-3-3ζ belongs to the 14-3-3 protein family, which is a class of highly conserved acidic proteins encoded by seven mammalian genes (α/β, ε, η, γ, τ/θ, ζ/δ, and σ) (21, 22). These seven isoforms share about 50% amino acid identity; nevertheless, UTKO1 seems to bind somewhat selectively to the ζ isomer (Fig. 4*C*). This selectivity can be explained by our finding that UTKO1 bound to the C-terminal region of 14-3-3ζ (supplemental Fig. S3), because this segment is the most variable region of the 14-3-3 isoforms (31). Taken together, these results suggest that 14-3-3ζ is involved in the mechanism for only the second EGF-induced wave of Rac1 activation. Moreover, UTKO1 bound to and inactivated 14-3-3ζ, thereby inhibiting the second EGF-induced wave of Rac1 activation. However, we cannot exclude the possibility that other members of the 14-3-3 family are also related to the inhibition of the second EGF-induced wave of Rac1 activation caused by UTKO1.

What had remained unclear was the mechanism for the involvement of 14-3-3ζ in the second EGF-induced wave of

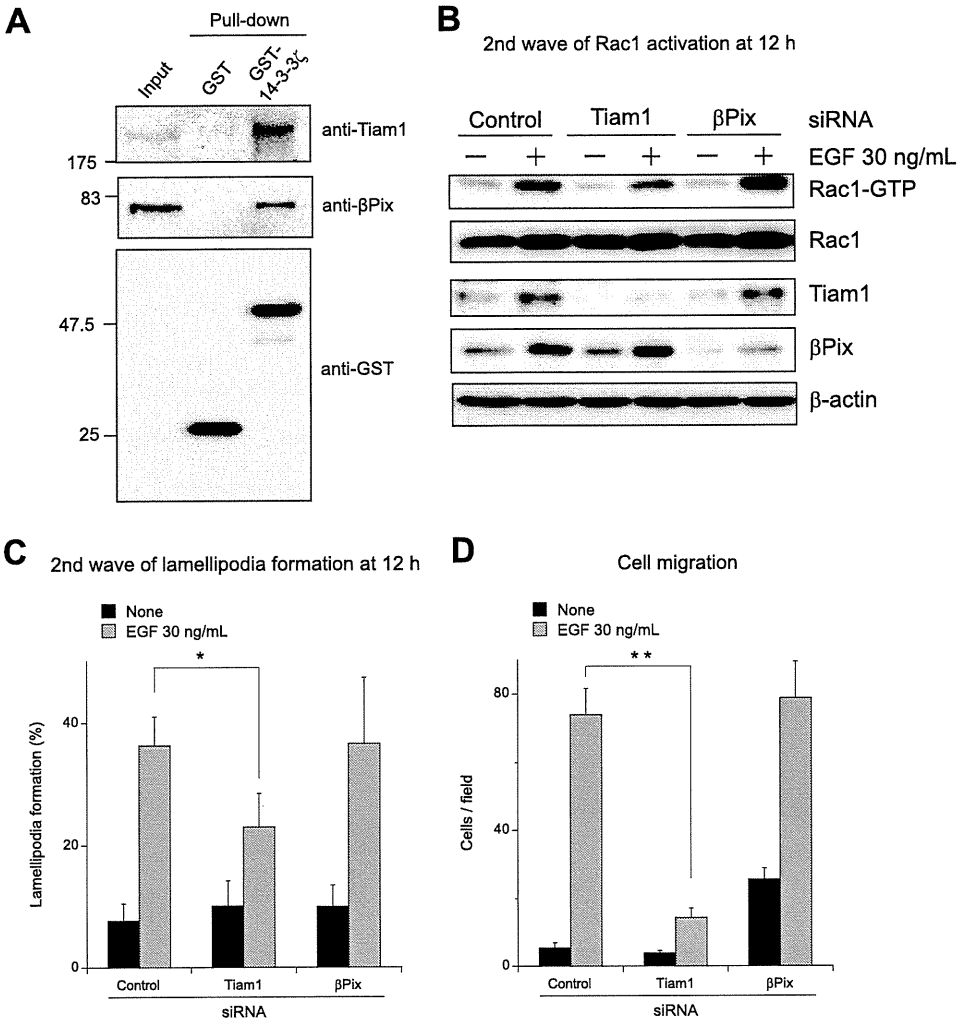

FIGURE 5. **Identification of Tiam1 as a RacGEF which is responsible for the second EGF-induced wave of Rac1 activation.** *A*, GST pulldown assay. Lysates of A431 cells stimulated with EGF for 12 h were incubated with GST or GST-14-3-3ζ and glutathione-Sepharose 4B. The precipitated proteins were subjected to Western blotting using the indicated antibodies. *B–D*, knockdown experiments. *B* and *C*, control, Tiam1, or βPix siRNA-transfected A431 cells were stimulated with EGF for 12 h. Then the cells were examined for active Rac1 by pulldown assay (*B*) or the cells with lamellipodia were counted (*C*). The data represent the means ± S.D. ($n = 6$). *D*, control, Tiam1, or βPix siRNA-transfected A431 cells were incubated in the upper chamber and stimulated with or without EGF for 24 h. Then the migrated cells were counted. The data represent the means ± S.D. ($n = 5$). For *C* and *D*, statistical analyses were performed with a two-tailed Student's *t* test. *, $p = 0.0036$; **, $p = 5.9 \times 10^{-9}$. Throughout, the data were representative of at least three independent studies. For *C*, more than 300 cells were analyzed per experiment.

Rac1 activation and how UTKO1 binding to 14-3-3ζ related to the suppression of the second wave. 14-3-3 proteins function as molecular scaffolds by modulating the conformation of their binding partners; therefore, we speculated that the binding partner of 14-3-3ζ would regulate the second EGF-induced wave of Rac1 activation. Of more than 200 known binding partners of 14-3-3 proteins (25, 32, 33), Tiam1 has been reported to be a Rac-specific GEF (34). Indeed, Tiam1 in lysates from A431 cells stimulated with EGF for 12 h was confirmed to co-precipitate with GST-14-3-3ζ (Fig. 5*A*). Knockdown of Tiam1 by siRNA was found to reduce the second EGF-induced wave of Rac1 activation but not the first wave (Fig. 5*B* and supplemental Fig. S4*A*). Interestingly, the intracellular expression level of Tiam1 is quite low in unstimulated A431 cells; it gradually increased and reached its zenith within 12 h after EGF stimulation (supplemental Fig. S6). These findings might explain why Tiam1 is not involved in the first wave of Rac1 activation. The involvement of Tiam1 in the second wave was further confirmed using NSC23766, a specific inhibitor of Tiam1-mediated activation of Rac1 (35, 36): NSC23766 inhibited both EGF-induced cell migration and second wave of Rac1 activation, but not the first wave (supplemental Fig. S7). Taken together with our finding that knockdown of 14-3-3ζ inhibited the second EGF-induced wave of Rac1 activation but not the first wave, the second wave would require interaction between 14-3-3ζ and Tiam1. This interaction was disrupted by the binding of UTKO1 to 14-3-3ζ (Fig. 6); therefore, UTKO1 inhibited the second wave of Rac1 activation by inhibiting the interaction between 14-3-3ζ and Tiam1.

Recently, it has been reported that the interaction of 14-3-3 proteins with the N terminus of Tiam1 regulates its protein stability (37). However, UTKO1 affected neither the stability of Tiam1 protein nor the intracellular localization of Tiam1 in our assay system (supplemental Fig. S8). Therefore, it is likely that conformational change of Tiam1 caused by interaction with

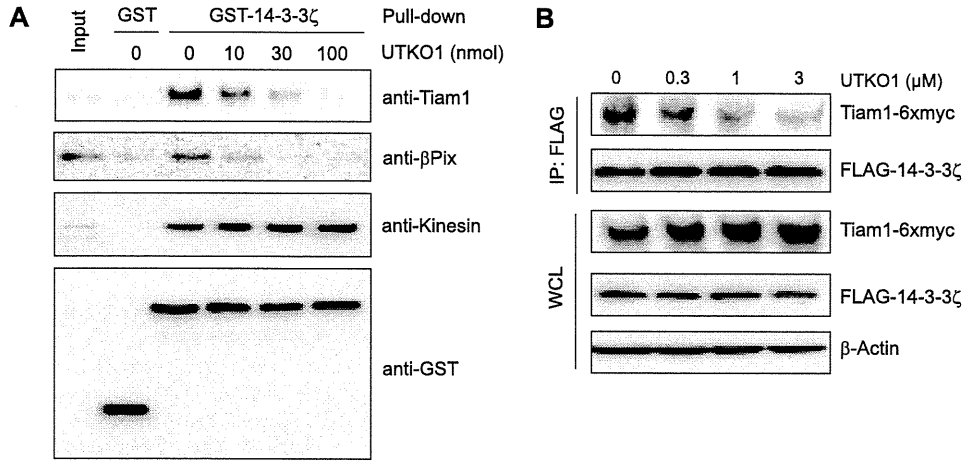

FIGURE 6. **UTKO1 inhibits the binding of 14-3-3ζ to Tiam1.** *A*, GST pulldown assay. Lysates of A431 cells stimulated with EGF for 12 h were incubated with purified GST or GST-14-3-3ζ in the absence or presence of UTKO1. The binding proteins of GST or GST-14-3-3ζ precipitated with glutathione-Sepharose 4B were subjected to Western blotting using the indicated antibodies. *B*, immunoprecipitation assay. FLAG-14-3-3ζ-expressing A431 cells were transiently transfected with Tiam1-6×Myc. After 24 h, the cells were stimulated with EGF for 12 h in the absence or presence of UTKO1. The cells were lysed, and the protein complexes were precipitated with anti-FLAG antibody. The immunoprecipitants were subjected to Western blotting using the indicated antibodies. Throughout, the data were representative of at least three independent studies.

14-3-3ζ activates the GEF property of Tiam1 and is inhibited by UTKO1. However, Tiam1 is not the only GEF regulating the second wave of Rac1 activation, because partial activation of second wave Rac1 was still observed in Tiam1 knockdown A431 cells. Therefore, another RacGEF might be involved in second wave Rac1 activation, possibly also through an interaction with 14-3-3ζ.

βPix, another RacGEF, has also been reported to be a 14-3-3 binding partner (19, 32), and we confirmed the interaction between βPix and 14-3-3ζ. However, knockdown of βPix did not affect the second EGF-induced wave of Rac1 activation but rather enhanced it even when the cells were not stimulated with EGF (Fig. 5*B* and supplemental Fig. S5*C*). Therefore, although UTKO1 disrupted the interaction of 14-3-3ζ with βPix (Fig. 6*A*), this disruption is not responsible for the UTKO1-inhibited second wave of Rac1 activation.

Among the multiple GEFs, Asef and Vav2 have been shown to activate Rac1 in response to EGF (18, 38). However, in most reported experiments, Rac1 activation was detected only within minutes of EGF stimulation (12, 18, 38, 39). We did not detect any interaction between 14-3-3ζ and Asef or Vav2 at times corresponding to the first or second wave following EGF stimulation (supplemental Fig. S9). Therefore, it is likely that Asef and Vav2 function as RacGEF during the first wave of Rac1 activation but are not involved in the 14-3-3ζ-mediated EGF-induced wave of Rac1 activation. Moreover, we cannot exclude the possibility that a 14-3-3 binding partner other than RacGEF is responsible for the second wave of Rac1 activation.

The biphasic timing of Rac1 activation mirrors the biphasic formation of lamellipodia. The first wave of lamellipodia formation seems to be nonpolarized, but second wave lamellipodia are formed at the leading edge and polarized. Moreover, because inhibition of only the second wave of Rac1 activation by UTKO1, as well as NSC23766, is enough to inhibit cell migration, the second wave is required for EGF-induced cell migration. The precise role of each wave of Rac1 activation in EGF-induced cell migration is being actively investigated.

Acknowledgments—We thank Dr. M. Yoshida and Dr. A. Ito for the LC-MS/MS analysis (RIKEN, Japan) and Dr. H. Sugimura for kindly providing plasmid (Hamamatsu University School of Medicine, Japan).

REFERENCES

1. Lauffenburger, D. A., and Horwitz, A. F. (1996) *Cell* **84,** 359–369
2. Pollard, T. D., and Borisy, G. G. (2003) *Cell* **112,** 453–465
3. Small, J. V., Stradal, T., Vignal, E., and Rottner, K. (2002) *Trends Cell Biol.* **12,** 112–120
4. Yamazaki, D., Suetsugu, S., Miki, H., Kataoka, Y., Nishikawa, S., Fujiwara, T., Yoshida, N., and Takenawa, T. (2003) *Nature* **424,** 452–456
5. Blanchoin, L., Amann, K. J., Higgs, H. N., Marchand, J. B., Kaiser, D. A., and Pollard, T. D. (2000) *Nature* **404,** 1007–1011
6. Takenawa, T., and Miki, H. (2001) *J. Cell Sci.* **114,** 1801–1809
7. Ridley, A. J., and Hall, A. (1992) *Cell* **70,** 389–399
8. Nobes, C. D., and Hall, A. (1995) *Cell* **81,** 53–62
9. Ridley, A. J., Paterson, H. F., Johnston, C. L., Diekmann, D., and Hall, A. (1992) *Cell* **70,** 401–410
10. Kaibuchi, K., Kuroda, S., and Amano, M. (1999) *Annu. Rev. Biochem.* **68,** 459–486
11. Takai, Y., Sasaki, T., and Matozaki, T. (2001) *Physiol. Rev.* **81,** 153–208
12. Kurokawa, K., Itoh, R. E., Yoshizaki, H., Nakamura, Y. O., and Matsuda, M. (2004) *Mol. Biol. Cell* **15,** 1003–1010
13. Takemoto, Y., Watanabe, H., Uchida, K., Matsumura, K., Nakae, K., Tashiro, E., Shindo, K., Kitahara, T., and Imoto, M. (2005) *Chem. Biol.* **12,** 1337–1347
14. Sawada, M., Kubo, S., Matsumura, K., Takemoto, Y., Kobayashi, H., Tashiro, E., Kitahara, T., Watanabe, H., and Imoto, M. (2011) *Bioorg. Med. Chem. Lett.* **21,** 1385–1389
15. Jones, G. E., Allen, W. E., and Ridley, A. J. (1998) *Cell Adhes. Commun.* **6,** 237–245
16. Chinkers, M., McKanna, J. A., and Cohen, S. (1979) *J. Cell Biol.* **83,** 260–265
17. Burridge, K., and Wennerberg, K. (2004) *Cell* **116,** 167–179
18. Itoh, R. E., Kiyokawa, E., Aoki, K., Nishioka, T., Akiyama, T., and Matsuda, M. (2008) *J. Cell Sci.* **121,** 2635–2642
19. Angrand, P. O., Segura, I., Völkel, P., Ghidelli, S., Terry, R., Brajenovic, M.,

Vintersten, K., Klein, R., Superti-Furga, G., Drewes, G., Kuster, B., Bouwmeester, T., and Acker-Palmer, A. (2006) *Mol. Cell Proteomics* **5,** 2211–2227
20. Deakin, N. O., Bass, M. D., Warwood, S., Schoelermann, J., Mostafavi-Pour, Z., Knight, D., Ballestrem, C., and Humphries, M. J. (2009) *J. Cell Sci.* **122,** 1654–1664
21. Aitken, A., Jones, D., Soneji, Y., and Howell, S. (1995) *Biochem. Soc. Trans.* **23,** 605–611
22. Rittinger, K., Budman, J., Xu, J., Volinia, S., Cantley, L. C., Smerdon, S. J., Gamblin, S. J., and Yaffe, M. B. (1999) *Mol. Cell* **4,** 153–166
23. Biyasheva, A., Svitkina, T., Kunda, P., Baum, B., and Borisy, G. (2004) *J. Cell Sci.* **117,** 837–848
24. van Hemert, M. J., Steensma, H. Y., and van Heusden, G. P. (2001) *Bioessays* **23,** 936–946
25. Pozuelo Rubio, M., Geraghty, K. M., Wong, B. H., Wood, N. T., Campbell, D. G., Morrice, N., and Mackintosh, C. (2004) *Biochem. J.* **379,** 395–408
26. O'Toole, T. E., Bialkowska, K., Li, X., and Fox, J. E. (2011) *J. Cell Physiol.* **226,** 2965–2978
27. Jones, S. M., and Kazlauskas, A. (2001) *Nat. Cell Biol.* **3,** 165–172
28. Jones, S. M., Klinghoffer, R., Prestwich, G. D., Toker, A., and Kazlauskas, A. (1999) *Curr. Biol.* **9,** 512–521
29. Lee, S. H., Kunz, J., Lin, S. H., and Yu-Lee, L. Y. (2007) *Cancer Res.* **67,** 11045–11053
30. Koivusalo, M., Welch, C., Hayashi, H., Scott, C. C., Kim, M., Alexander, T., Touret, N., Hahn, K. M., and Grinstein, S. (2010) *J. Cell Biol.* **188,** 547–563
31. Gardino, A. K., Smerdon, S. J., and Yaffe, M. B. (2006) *Semin. Cancer Biol.* **16,** 173–182
32. Jin, J., Smith, F. D., Stark, C., Wells, C. D., Fawcett, J. P., Kulkarni, S., Metalnikov, P., O'Donnell, P., Taylor, P., Taylor, L., Zougman, A., Woodgett, J. R., Langeberg, L. K., Scott, J. D., and Pawson, T. (2004) *Curr. Biol.* **14,** 1436–1450
33. Meek, S. E., Lane, W. S., and Piwnica-Worms, H. (2004) *J. Biol. Chem.* **279,** 32046–32054
34. Habets, G. G., Scholtes, E. H., Zuydgeest, D., van der Kammen, R. A., Stam, J. C., Berns, A., and Collard, J. G. (1994) *Cell* **77,** 537–549
35. Gao, Y., Dickerson, J. B., Guo, F., Zheng, J., and Zheng, Y. (2004) *Proc. Natl. Acad. Sci. U.S.A.* **101,** 7618–7623
36. Veluthakal, R., Madathilparambil, S. V., McDonald, P., Olson, L. K., and Kowluru, A. (2009) *Biochem. Pharmacol.* **77,** 101–113
37. Woodcock, S. A., Jones, R. C., Edmondson, R. D., and Malliri, A. (2009) *J. Proteome Res.* **8,** 5629–5641
38. Marcoux, N., and Vuori, K. (2003) *Oncogene* **22,** 6100–6106
39. Sini, P., Cannas, A., Koleske, A. J., Di Fiore, P. P., and Scita, G. (2004) *Nat. Cell Biol.* **6,** 268–274

The Journal of Antibiotics (2011) 64, 361–366

www.nature.com/ja

ORIGINAL ARTICLE

Mycotrienin II, a translation inhibitor that prevents ICAM-1 expression induced by pro-inflammatory cytokines

Yuriko Yamada[1], Etsu Tashiro[2], Shigeru Taketani[1], Masaya Imoto[2] and Takao Kataoka[1]

Pro-inflammatory cytokines, such as tumor necrosis factor (TNF)-α and interleukin-1α (IL-1α), trigger the activation of the transcription factor nuclear factor-κB, a molecule that induces the expression of a variety of genes, including intercellular adhesion molecule-1 (ICAM-1). Here, we report that mycotrienin II, a member of the triene-ansamycin group, inhibited the cell-surface ICAM-1 expression induced by TNF-α more strongly than that induced by IL-1α in human lung carcinoma A549 cells. Mycotrienin II was found to inhibit protein synthesis in intact living cells, as well as in cell-free translation systems. Among translation inhibitors tested, acetoxycycloheximide and anisomycin, but neither puromycin nor emetine, inhibited the TNF-α-induced ICAM-1 expression at lower concentrations than the IL-1α-induced ICAM-1 expression. Several compounds of the triene-ansamycin group (that is, mycotrienin I, trienomycin A, trierixin, quinotrierixin and quinotrierixin HQ) also inhibited ICAM-1 expression, as well as cell-free translation in a manner similar to mycotrienin II. These results indicate that mycotrienin II is a direct inhibitor of translation, thereby inhibiting ICAM-1 expression induced by pro-inflammatory cytokines.
The Journal of Antibiotics (2011) **64**, 361–366; doi:10.1038/ja.2011.23; published online 30 March 2011

Keywords: ICAM-1; IL-1α; mycotrienin II; NF-κB; pro-inflammatory cytokine; TNF-α; triene-ansamycin

INTRODUCTION

Pro-inflammatory cytokines, such as tumor necrosis factor (TNF)-α and interleukin-1α (IL-1α), induce the expression of a variety of genes essential for inflammatory responses, such as intercellular adhesion molecule-1 (ICAM-1; CD54).[1] ICAM-1 is a cell-surface glycoprotein that binds to lymphocyte function-associated antigen-1 (CD11a/CD18) and Mac-1 (CD11b/CD18).[2] As one of its physiological roles, ICAM-1 inducibly expressed on vascular endothelial cells is required for the recruitment of leukocytes via the interaction with lymphocyte function-associated antigen-1 or Mac-1 and their subsequent transmigration to inflamed sites.[3,4] ICAM-1 expression is known to be induced primarily by the transcription factor nuclear factor-κB.[1] So far, many small molecules targeting the nuclear factor-κB signaling pathway induced by pro-inflammatory cytokines have been identified.[5]

Mycotrienin II (Figure 1a) was isolated from *Streptomyces* sp. and belongs to the triene-ansamycin group of compounds.[6,7] Mycotrienin II possesses various biological activities in mammalian cells, such as cytotoxicity and inhibition of osteoclastic bone resorption and endoplasmic reticulum (ER) stress-induced X-box binding protein 1 activation.[8–13] In the course of our screening for anti-inflammatory agents, we found that mycotrienin II inhibits ICAM-1 expression induced by TNF-α and IL-1α. In this study, we further investigated the molecular mechanism underlying the inhibition of ICAM-1 expression by mycotrienin II.

MATERIALS AND METHODS

Cell culture

Human lung carcinoma A549 cells were provided by the Health Science Research Resources Bank (Tokyo, Japan). A549 cells were maintained in RPMI 1640 medium (Invitrogen, Carlsbad, CA, USA) supplemented with 10% (v/v) heat-inactivated fetal calf serum (JRH Biosciences, Lenexa, KS, USA) and penicillin-streptomycin mixed solution (Nacalai Tesque, Kyoto, Japan).

Reagents

Recombinant human TNF-α and human IL-1α were kindly provided by Dainippon Pharmaceutical (Osaka, Japan). Mycotrienin I, mycotrienin II, trienomycin A, trierixin and quinotrierixin were isolated from the culture broth of *Streptomyces* sp. PAE37.[13] Quinotrierixin HQ, 13–ketomycotrienin I and 13–ketomycotrienin II were prepared as described previously.[13] Acetoxycycloheximide was isolated from the culture broth of an unidentified actinomycete strain designated by ML44-113F2.[14] Anisomycin and cycloheximide were purchased from Wako Pure Chemical Industries (Osaka, Japan). Emetine and puromycin were obtained from Sigma-Aldrich (St Louis, MO, USA).

[1]Department of Applied Biology, Kyoto Institute of Technology, Matsugasaki, Sakyo-ku, Kyoto, Japan and [2]Department of Biosciences and Informatics, Faculty of Science and Technology, Keio University, Yokohama, Japan
Correspondence: Dr T Kataoka, Department of Applied Biology, Kyoto Institute of Technology, Matsugasaki, Kyoto 606-8585, Japan.
E-mail: takao.kataoka@kit.ac.jp
Received 3 December 2010; revised 14 February 2011; accepted 17 February 2011; published online 30 March 2011

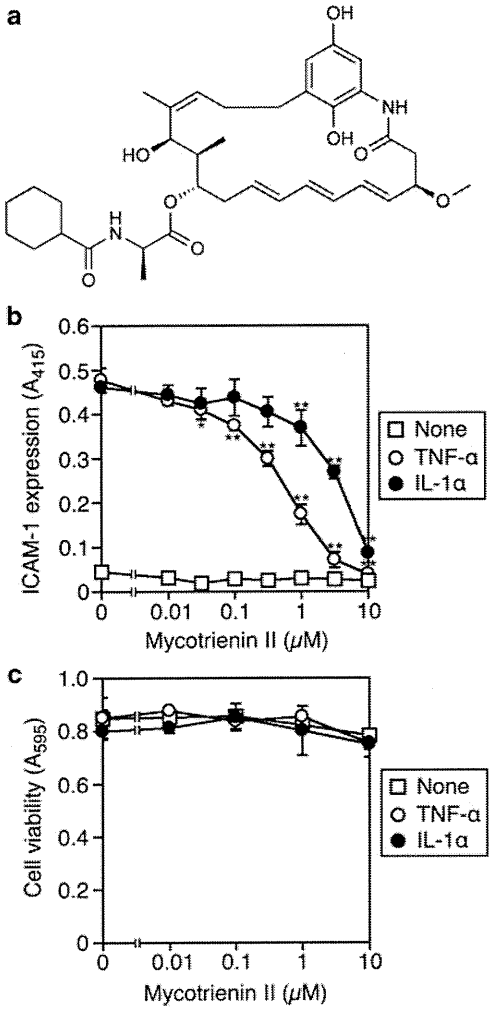

Figure 1 Mycotrienin II inhibits cell-surface intercellular adhesion molecule-1 (ICAM-1) expression induced by tumor necrosis factor-α (TNF-α) and interleukin-1α (IL-1α). (**a**) Structure of mycotrienin II. (**b**) A549 cells were pretreated with various concentrations of mycotrienin II for 1 h and then incubated with TNF-α (2.5 ng ml^{-1}; open circles) or IL-1α (0.25 ng ml^{-1}; filled circles) or without cytokines (open squares) for 6 h in the presence of mycotrienin II. ICAM-1 expression (A_{415}) is shown as means ± s.d. (n=3). *P<0.05 and **P<0.01, compared with control. Data are representative of two independent experiments. (**c**) A549 cells were incubated with various concentrations of mycotrienin II for 1 h and then incubated with TNF-α (2.5 ng ml^{-1}; open circles) or IL-1α (0.25 ng ml^{-1}; filled circles) or without cytokines (open squares) for 6 h in the presence of mycotrienin II. Cell viability (A_{595}) is shown as means ± s.d. (n=3). *P<0.05 and **P<0.01, compared with control. Data are representative of two independent experiments.

Assay for cell-surface expression of ICAM-1

A549 cells were washed twice with phosphate-buffered saline (PBS) and fixed with 1% paraformaldehyde–PBS for 15 min. After washing twice with PBS, the cells were incubated with 1% bovine serum albumin (Sigma-Aldrich)–PBS overnight. Fixed cells were treated with mouse anti-human ICAM-1 IgG antibody (clone 15.2; Leinco Technologies, St Louis, MO, USA) for 60 min and then washed three times with 0.02% Tween 20–PBS. The cells were further treated with horseradish peroxidase-linked anti-mouse IgG antibody (Jackson Immunoresearch, West Grove, PA, USA) for 60 min and then washed three times with 0.02% Tween-20–PBS. To develop the colorimetric reaction, the cells were incubated with the substrate solution (0.2 M sodium citrate (pH 5.3), 0.1% *o*-phenylenediamine dihydrochloride, 0.02% H_2O_2) for 20 min at 37 °C. Absorbance at 415 nm was measured with a Model 680 microplate reader (Bio-Rad Laboratories, Hercules, CA, USA).

Assay for cell viability

A549 cells were pulsed with MTT (3-(4,5-dimethylthiazol-2-yl)-2,5-diphenyltetrazolium bromide, 500 μg ml^{-1}) for 4 h and resultant MTT formazan was solubilized with 5% sodium dodecyl sulfate overnight. Absorbance at 595 nm was measured with a Model 680 microplate reader (Bio-Rad Laboratories).

Assay for macromolecular synthesis

A549 cells were pulse-labeled with [4,5-^{3}H]L-leucine (41.66 TBq mmol^{-1}; Moravek Biochemicals, Brea, CA, USA), [methyl-^{3}H]thymidine (2.37 TBq mmol^{-1}; MP Biomedicals, Santa Ana, CA, USA), and [5-^{3}H]uridine (0.626 TBq mmol^{-1}; Moravek Biomedicals) for the indicated times. The labeled cells were washed three times with PBS and then lysed with 250 mM NaOH for 15 min, followed by 1 h incubation on ice in the presence of 5% trichloroacetic acid. The precipitates and the supernatants were separated by centrifugation (10 000×*g*, 5 min). Radioactivity was measured with a 1900CA TRI-CARB liquid scintillation analyzer (Packard Instrument, Meriden, CT, USA).

Assay for cell-free protein synthesis

The T7-driven luciferase cDNA was subjected to the cell-free reaction (30 °C, 90 min) for transcription and translation by the TnT T7 Coupled Reticulocyte Lysate Systems (Promega, Madison, WI, USA). Luciferase mRNA was subjected to the cell-free reaction (30 °C, 90 min) for translation by the Rabbit Reticulocyte Lysate System (Promega). Reaction mixtures were mixed with the luciferase assay solution and relative light units were immediately measured with a Lumitester K-100 Luminometer (Hamamatsu Photonics, Hamamatsu, Japan).

Statistical analysis

Statistical significance was assessed by one-way analysis of variance, followed by the Tuker test for multiple comparisons using KaleidaGraph (Synergy Software, Reading, PA, USA). Differences of P<0.05 were considered to be statistically significant.

RESULTS

Mycotrienin II inhibits cell-surface ICAM-1 expression induced by TNF-α and IL-1α

Pro-inflammatory cytokines, such as TNF-α or IL-1α, induce the expression of various cell-surface molecules during inflammatory responses.[1] Upon stimulation with TNF-α or IL-1α, lung carcinoma A549 cells expressed ICAM-1 on their cell surface. Mycotrienin II was found to inhibit the cell-surface ICAM-1 expression induced by TNF-α and IL-1α in a dose-dependent manner (Figure 1b). As its characteristic inhibitory profiles, the TNF-α-induced ICAM-1 expression (IC_{50} value: 0.3 μM) was more strongly inhibited by mycotrienin II than the IL-1α-induced ICAM-1 expression (IC_{50} value: 3.1 μM). During the same incubation time, mycotrienin II exerted a marginal effect on cell viability up to 10 μM even in the presence of TNF-α or IL-1α (Figure 1c). Consistent with these data, mycotrienin II did not induce the release of L-lactose dehydrogenase into the culture medium in the presence or absence of TNF-α or IL-1α (data not shown). These results indicate that the inhibition of cell-surface ICAM-1 expression by mycotrienin II is not likely to be nonspecific cytotoxicity and induction of cell death.

Mycotrienin II inhibits cellular and cell-free translation

Recently, it has been shown by us and other group that the trine-ansamycin group compounds, such as cytotrienin A and quinotrierixin, are translation inhibitors.[15,16] To investigate whether mycotrienin